EFFECTS OF CYCLIC LOADING ON PEAK SHEAR STRENGTH OF ROCK JOINTS

Thanakorn Kamonpet

A Thesis Submitted in Partial Fulfillment of the Requirements for the

Degree of Master of Engineering in Geotechnology

Suranaree University of Technology

Academic Year 2012

ผลกระทบของแรงแบบวัฏจักรต่อกำลังเฉือนสูงสุดของรอยแตกในหิน

นายธนากร กมลเพชร

วิทยานิพนธ์นี้เป็นส่วนหนึ่งของการศึกษาตามหลักสูตรปริญญาวิศวกรรมศาสตรมหาบัณฑิต
สาขาวิชาเทคโนโลยีธรณี
มหาวิทยาลัยเทคโนโลยีสุรนารี
ปีการศึกษา 2555

EFFECTS OF CYCLIC LOADING ON PEAK SHEAR STRENGTH OF ROCK JOINTS

Suranaree University of Technology has approved this thesis submitted in partial fulfillment of the requirements for a Master's Degree.

Thesis Examining Committee

_____

(Assoc. Prof. Kriangkrai Trisarn)

Chairperson

_____

(Assoc. Prof. Dr. Kittitep Fuenkajorn)

Member (Thesis Advisor)

_____

(Dr. Decho Phueakphum)

Member

_____

(Prof. Dr. Sukit Limpijumnong)

Vice Rector for Academic Affairs

_____

(Assoc. Prof. Flt. Lt. Dr. Kontorn Chamniprasart)

Dean of Institute of Engineering

ธนากร กมลเพชร : ผลกระทบของแรงแบบวัฏจักรต่อกำลังเฉือนสูงสุดของรอยแตกในหิน (EFFECTS OF CYCLIC LOADING ON PEAK SHEAR STRENGTH OF ROCK JOINTS) อาจารย์ที่ปรึกษา : รองศาสตราจารย์ ดร.กิตติเทพ เฟื่องขจร, 57 หน้า.

วัตถุประสงค์ของการศึกษานี้คือเพื่อทดสอบพฤติกรรมของรอยแตกในหินภายใต้การให้แรงเฉือนแบบวัฏจักร การทดสอบความเค้นเฉือนโดยตรงดำเนินการเพื่อหาค่ากำลังรับแรงเฉือนสูงสุดและกำลังรับแรงเฉือนคงเหลือของรอยแตกในตัวอย่างหินทรายชุดภูพาน หินปูนชุดสระบุรี และหินแกรนิตชุดสระบุรี รอยแตกได้ถูกทำขึ้นภายในห้องปฏิบัติการซึ่งมีสองชนิดคือ รอยแตกแบบผิวขรุขระโดยวิธีการให้แรงดึงและรอยแตกแบบผิวเรียบโดยการตัด การทดสอบได้มีการให้แรงเฉือนจำนวน 10 วัฏจักรภายใต้ความเค้นตั้งฉากที่ผันแปรตั้งแต่ 0.5 1 2 3 ถึง 4 MPa ผลการทดสอบระบุว่าการให้แรงเฉือนแบบวัฏจักรเป็นตัวแปรที่สำคัญในการลดความเสียดทานของรอยแตกในหิน ซึ่งตัวอย่างหินทั้งหมดที่ทำการทดสอบการให้แรงเฉือนในวัฏจักรแรกมีค่ามุมเสียดทานประมาณ 50 องศา และจะลดลงเหลือประมาณ 40 องศา ในวัฏจักรถัดมาและไม่มีการเปลี่ยนแปลงมากจากวัฏจักรที่ 2 ถึงวัฏจักรที่ 10 ในส่วนของค่าความเค้นยึดติดของรอยแตกที่ได้จากวัฏจักรแรกมีค่า 0.43-1.56 เมกกะปาสคาล และลดลงเหลือ 0.34-0.38 เมกกะปาสคาล ในวัฏจักรที่ 2 ถึงวัฏจักรที่ 10 และค่าความเหนียวของรอยแตกลดลงจาก 2.0-6.5 เมกกะปาสคาลต่อมิลลิเมตรในวัฏจักรแรก เหลือ 0.7-5.4 เมกกะปาสคาลต่อมิลลิเมตรในวัฏจักรที่ 2 ถึงวัฏจักรที่ 10 โดยส่วนใหญ่การกร่อนของผิวขรุขระของรอยแตกจะมีมากหลังจากการให้แรงเฉือนในวัฏจักรแรก และสามารถสรุปได้ว่าการทดสอบการให้แรงเฉือนแบบวัฏจักรไม่มีผลกระทบกับรอยแตกแบบผิวเรียบ ซึ่งแสดงถึงปัจจัยหลักที่มีผลกับการทดสอบการให้แรงเฉือนแบบวัฏจักรคือระดับของความขรุขระและค่าความแข็งของผิวรอยแตกในตัวอย่างหิน

สาขาวิชา เทคโนโลยีธรณี ลายมือชื่อนักศึกษา _____

ปีการศึกษา 2555 ลายมือชื่ออาจารย์ที่ปรึกษา _____

THANAKORN KAMONPET : EFFECTS OF CYCLIC LOADING ON PEAK SHEAR STRENGTH OF ROCK JOINTS. THESIS ADVISOR : ASSOC. PROF. KITTITEP FUENKAJORN, Ph.D., P.E., 57 PP.

JOINT/CYCLIC LOADING/SHEAR STRENGTH/AMPLITUDE

The objective of this study is to experimentally determine the behavior of rock fractures under cyclic shear loading. Direct shear tests have been performed to determine the peak and residual shear strengths of tension-induced fractures in Phu Phan sandstone, Saraburi limestone, and Saraburi granite. The fractures are artificially made in the laboratory by tension inducing and saw cut methods. The cyclic shear loads are applied up to ten cycles. The normal stresses are varied from 0.5, 1, 2, 3, to 4 MPa. Results indicate that the cyclic shear stresses can significantly reduce the fracture shear strength and shear stiffness. The friction angles measured from all tested rocks are about 50° at first cycle and decrease to 40° for the second to tenth cycles. The cohesion reduces from 0.43-1.56 MPa for the first cycle to 0.34-0.38 MPa for cycles 2 through 10. The shear stiffness decreases from 2.0-6.5 MPa/mm for the first cycle to 0.7-5.4 MPa/mm for cycles 2 through 10. Degradation of the asperities mainly occurs after the first cycle. The shear strengths of the saw cut surfaces are independent of the loading cycle, which implies that the main factor that controls the effect of cyclic shear loading is the fracture roughness and rock strength on the fracture wall.

School of Geotechnology Student's Signature_____

Academic Year 2012 Advisor's Signature_____

ACKNOWLEDGEMENTS

The author wishes to acknowledge the support from the Suranaree University of Technology (SUT) who has provided funding for this research.

Grateful thanks and appreciation are given to Assoc. Prof. Dr. Kittitep Fuenkajorn, thesis advisor, who lets the author work independently, but gave a critical review of this research. Many thanks are also extended to Assoc. Prof. Kringkrai Trisarn and Dr. Decho Phueakphum, who served on the thesis committee and commented on the manuscript.

Finally, I most gratefully acknowledge my parents and friends for all their supported throughout the period of this research.

Thanakorn Kamonpet

TABLE OF CONTENTS

Page

TABLE OF CONTENTS (Continued)

Page

TABLE OF CONTENTS (Continued)

Page

LIST OF TABLES

Table **Page**

LIST OF FIGURES

Figure **Page**

LIST OF FIGURES (Continued)

Figure **Page**

LIST OF FIGURES (Continued)

Figure **Page**

SYMBOLS AND ABBREVIATIONS

κ	=	Empirical constant for equation (5.1)
τ	=	Shear stress
ϕ_p	=	Peak friction angle
τ_p	=	Peak shear strength
ϕ_r	=	Residual friction angle
τ_r	=	Residual shear strength
A	=	Contact area during shear test
c	=	Cohesion
d_n	=	Normal displacement
d_s	=	Shear displacement
JRC	=	Joint roughness coefficient
K_n	=	Joint normal stiffness
K_s	=	Joint shear stiffness
P_p	=	Maximum shear force
P_r	=	Residual shear force
R	=	Coefficient of correlation
α	=	Empirical constant for equation (5.3)

SYMBOLS AND ABBREVIATIONS (Continued)

β	=	Empirical constant for equation (5.3)
σ_n	=	Normal stress
ω	=	Empirical constant for equation (5.1)

CHAPTER I

INTRODUCTION

1.1 Rationale and background

Fracture shear strength is one of the key properties used in the stability analysis and design of engineering structures in rock mass, e.g. slopes, tunnels and foundations. The conventional method currently used to determine the fracture shear strength is the direct shear testing which can be performed in the laboratory. The joint properties such as roughness, strength of asperities, separation, gouge and even the spatial distributions make the behavior of jointed rock masses more complicated (Lee et al., 2001). Most of the previous laboratory experiments on the mechanical properties of rock joints have been focused on determining the peak shear strength and the stress–displacement relations under unidirectional shear loading. Shear displacements due to earthquake loadings can also affect the shear strength. The behavior of rock joints under cyclic loading depends on their surface properties (Jafari et al., 2003). Small repetitive earthquakes cannot make considerable movement, but because of their repetitive nature they may affect the shear resistance of rock joints (Jafari et al., 2002). During strong earthquakes, relative large cyclic displacements may occur between the walls of rock joints. These cyclic displacements can degrade the first and second order asperities along the joint surface and reduce the shear strength of rock joint (Hosseinu et al., 2004). The shear strength of rock joints due to cyclic loadings is therefore an important consideration for long-term stability of engineering structures in the areas where seismic activities occur.

The shear strength of rock joints due to cyclic loadings is an important consideration. Knowledge and understanding of the cyclic loading on the rock fractures shear strength are however rare.

1.2 Research objective

The objective of this study is to determine the behavior of rock fractures under cyclic loads in three rock types. The rock specimens are prepared from Phu Phan sandstone, Saraburi limestone, and Saraburi granite. The effort primarily involves performing series of cyclic direct shear tests on smooth surface and rough fractures in the laboratory. The peak and residual shear strengths, dilation rate and degradation of asperities of the fractures under cyclic shearing are of interest. The findings are of useful in understanding the fracture shear strength as affected by cycles of loading induced by blasting or seismic activities.

1.3 Research methodology

As shown in Figure 1.1, the research methodology comprises 6 steps including literature review, sample collection and preparation, laboratory testing, mathematical relations, discussions and conclusions, and thesis writing.

1.3.1 Literature review

Literature review is carried out to understand the fractures shear strength under cyclic loading. These include theories, test procedures, results, analysis and applications. The sources of information are from journals, technical reports and conference papers. A summary of the literature review is given in the thesis.

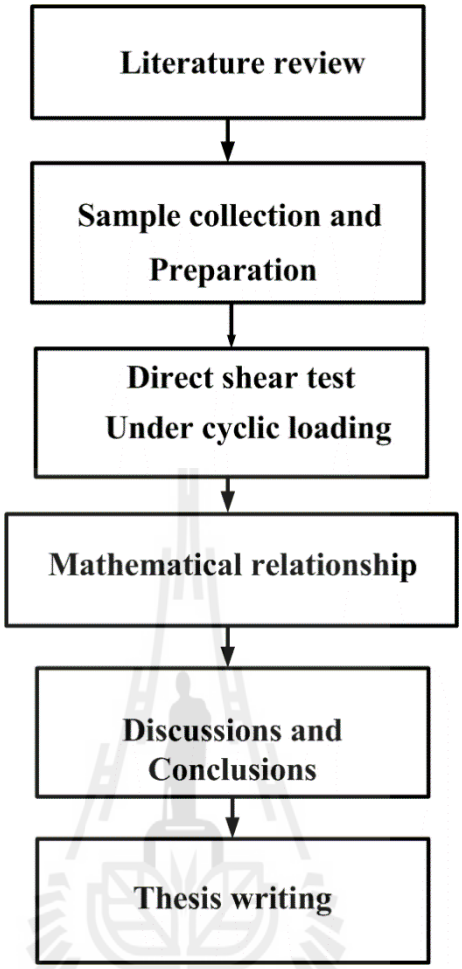

Figure 1.1 Research methodology.

1.3.2 Sample collection and preparation

Sample preparation is carried out in the laboratory at the Suranaree University of Technology. The rock samples include Phu Phan sandstone, Saraburi granite, and Saraburi limestone. Samples for shear strength of rock fractures under cyclic loading test are prepared to have fracture area of about 8×10 cm^2. The fractures are artificially made in the laboratory by saw-cutting and tension inducing method.

1.3.3 Laboratory testing

The prepared specimens of the three rock types have been tested in the laboratory**.** The test procedure follows as much as practical the ASTM D5607-08 standard practice. Each specimen is sheared only once for each normal stress using a direct shear machine (SBEL DR44). The direct shear machine with a maximum shear load of 30,000 lbs and maximum normal load of 10,000 lbs is used. A series of cyclic shear test were conducted using the smooth and rough surface specimens of Phu Phan sandstone, Saraburi granite, and Saraburi limestone. The specimen is placed in direct shear load frame which is used to applied normal stresses equal to 0.5, 1, 2, 3, and 4 MPa. The rates of shear displacement are 0.01–0.02 mm/s. The number of loading cycles is 10 with the maximum shear displacement of ±5 mm.

1.3.4 Mathematical relationship

Results from laboratory measurements in terms of the peak and residual shear strengths, dilation rate and degradation of asperities of the fractures under cyclic loading are used to formulate mathematical relations. The objective is to predict the friction angle and cohesion under loading cycle characteristics.

1.3.5 Discussions and conclusions

All results from laboratory tests will be discussion in terms of the adequacy and reliability. The results will be provided in the conclusions.

1.3.6 Thesis writing

All research activities, methods, and results are documented and complied in the thesis.

1.4 Scope and limitations of the study

The scope and limitations of the research include as follows.

- Laboratory experiments will be conducted on specimens from three samples including Phu Phan sandstone, and Saraburi granite, Saraburi limestone.
- Testing on fractures will be made under normal stresses varying from 0.5 to 4 MPa
- All tested fractures will be artificially made in the laboratory by saw-cutting and tension induced method.
- All tests will be conducted under ambient temperature.
- The number of load cycles and normal stress will be analyzed.
- The test will use minimum fracture areas of 8×10 cm^2.
- All tests will be performed under dry condition.

1.5 Thesis contents

Chapter I introduces the thesis by briefly describing rationale and background. The research objectives, methodology, scope and limitations are identified. **Chapter II** summarizes results of the literature review. **Chapter III** describes sample collection and preparation. **Chapter IV** describes the laboratory experiment and presents the results obtained from the laboratory testing. **Chapter V** presents the relationship between friction angles, joint normal and shear stiffness, dilation rate, and number of loading cycles. **Chapter VI** concludes the research results, and provides recommendations for future research studies.

CHAPTER II

LITERATURE REVIEW

2.1 Introduction

This chapter summarizes the results of literature review carried out to understand the shear strength of rock joint under static and cyclic loading. The topics reviewed here include the behaviour of rock joints under static and cyclic loading conditions, cyclic shear testing system, and effect of cyclic loading on fracture shear strength.

2.2 Literature review

Hosseini et al. (2004) state that during strong earthquakes, relative large cyclic displacements may be occurred between the different walls of rock joints. These cyclic displacements degrade the first and second order asperities along the joint surface and reduce shear strength of rock joint. In their experimental study, the variation of shear strength of rock joints during large cyclic displacement is investigated to simulate the effects of strong earthquakes on rock joints. Artificial jointed samples have been prepared adopting a developed moulding method using special mortar and tested in a direct shear apparatus under cyclic loading conditions. Two types of the joint surface have been prepared for all the tested replicas: saw-tooth and a real joint surface moulded from a fresh joint. Schematic views of these surfaces are shown in Figure 2.1. The tests have been performed in different levels of normal

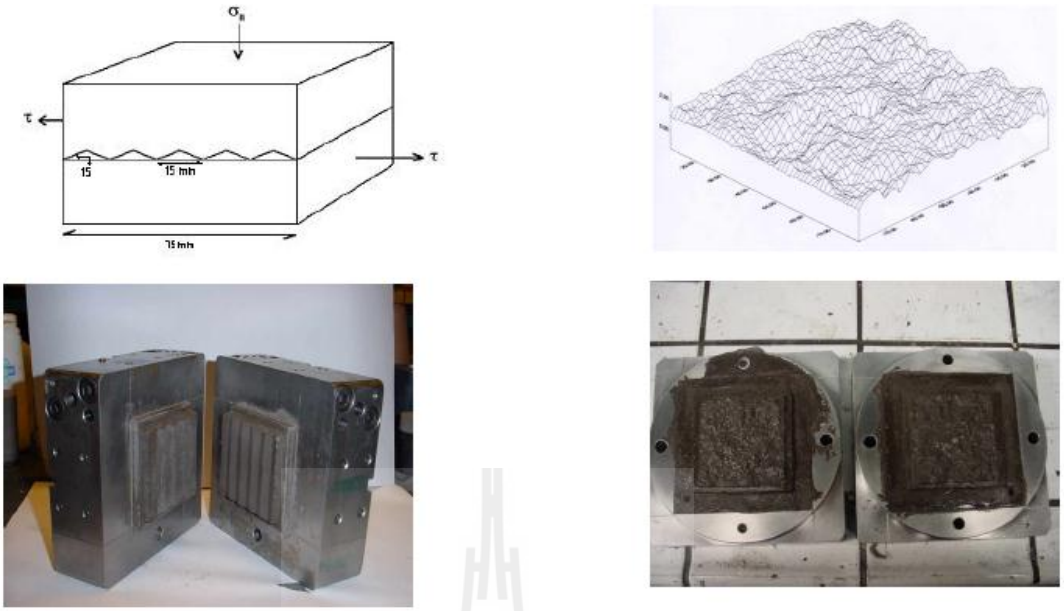

(a) (b)

Figure 2.1 (a) Saw-tooth samples and (b) real surface samples for direct shear test (Hosseini et al., 2004)

stresses to investigate the shearing behaviour of rock joints located at different depths from ground surface. In each test, several displacement cycles have been applied on the samples and the variation of shear strength, asperity degradation and wearing have been studied during each cycle. Based on the evaluations of experimental results, a mathematical model has been developed for prediction of shear strength in large cyclic loading conditions.

Jafari et al. (2003) observed the variation of the shear strengths of rock joints due to cyclic loadings. Identical joint surfaces were prepared using a developed moulding method with special mortar and shear tests performed under both static and cyclic loading conditions. Different levels of shear displacement were applied on the samples to study joint behaviour before and during considerable relative shear

displacement. It was found that the shear strength of joints was related to the rate of displacement (shearing velocity), number of loading cycles and stress amplitude. Finally, based on the experimental results, mathematical models were developed for evaluation of shear strength in cyclic loading conditions.

Based on the test results the following relation could be proposed for evaluating shear strength under low amplitude cyclic loading

$$\frac{\tau}{\sigma_n} = \frac{a(NC_s)^m(\omega_n A_n)^n}{1 + a(NC_s)^m(\omega_n A_n)^n} \tag{2.1}$$

Where τ is shear strength, σ_n is the normal stress, NC_s is the number of stress cycles, ω_n is the normalized shear velocity (normalized by the minimum shearing velocity during monotonic test, in which the maximum shear strength exists), A_n is normalized stress amplitude (normalized by maximum shear strength).

Based on calibration with the results of the tests performed, the following model parameters are obtained a = 0.3, m = -0.045 and n = -0.17

The parameter a is related to the mechanical properties of the joint sample (e.g. base friction angle, ϕ_b) and the geometrical features of joint surface. As the present investigations focused on artificial joint samples, more investigations on real rock joints with different conditions should be carried out to obtain a better evaluation of these parameters. The number of stress cycles, NC, has little effect on shear strength, represented by the small value for the parameter m: In contrast, stress amplitude and shearing velocity have relatively large effects on shear strength due to the higher value for the parameter n: As can be observed in Figure 2.2.

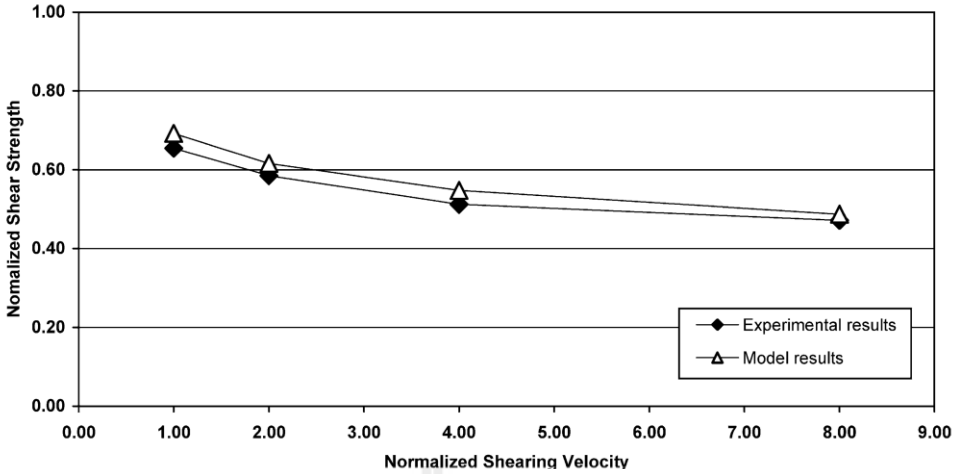

Figure 2.2 Comparison of the measured and calculated shear strength at different shear velocities (Jafari et al., 2003)

Souley et al. (1995) has studied joints in a given rock mass that are subjected to a wide variety of boundary conditions and also to various cycles of loading and unloading in both normal and shear directions. He presents an extension of the Saeb and Amadei model to take into account joint loading and unloading in both normal and shear directions. In the normal direction, the cyclic behavior is hyperbolic and the irrecoverable normal closure depends on the joint loading history. Concerning the shear direction change, two assumptions are supposed: the pre-peak behavior is elastic; and, during the residual behavior, the joint is smooth (all the asperities are crushed) and the shear band developed by these fragments is not taken into account.

Lee et al. (2001) proposed a cyclic shear testing system that was established to investigate the mechanical behavior of rough rock joints under cyclic loading conditions. Laboratory cyclic shear tests were conducted for two joint types of Hwangdeung granite and Yeosan marble, as shown in Figure 2.3, saw-cut and split tensile joints. Prior to the test, the roughness of each specimen was characterized by

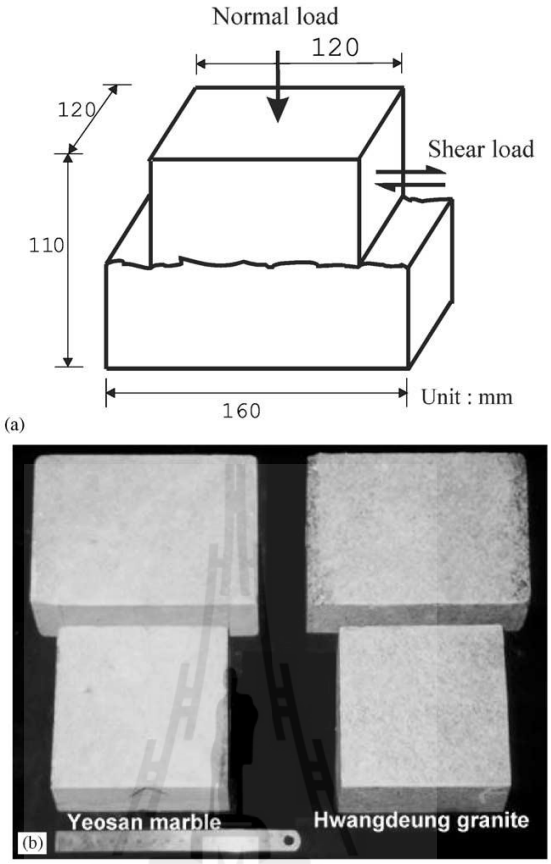

Figure 2.3 Joint specimens of Hwangdeung granite and Yeosan marble: (a) dimension of joint specimen and (b) upper and lower parts of joint specimens. (Lee et al., 2001)

measuring the surface topography using a laser profilometer. Several important aspects of cyclic joint behavior, such as high peak shear strength and non-linear dilation in the first loading cycle, different frictional resistance for the reversed shear loading direction, and anisotropic shear behavior and its dependence on the normal stress level were identified from the cyclic shear test results. These features and their variations in the subsequent loading cycles were mainly due to the effect of second order asperities and strength of rock material. It was also observed from experimental results that degradation of

asperities under cyclic shear loading also followed the exponential degradation laws for asperity angle and the mechanism for asperity degradation would be different depending upon the shearing direction and the type of asperities. Based on the experimental results an elasto-plastic constitutive model, which can consider the degradation of second order asperities, was proposed. Numerical simulations for the monotonic and cyclic shear loading indicated agreement with the laboratory test results.

Ma and Brady (1999) has studies the results from field observations of dynamic behaviour of an underground excavation compared with numerical studies of the rock deformation history. The field behaviour shows progressive accumulation of rock displacement and excavation deformation under successive episodes of dynamic loading. It is possible to reproduce the modes of rock response quite well using a distinct element model of the rock mass, but the way displacements develop is dependent on the joint model used in the analysis. It is suggested that, in rock masses subject to repeated dynamic loading, excavation design may need to take account of the prospect of the repeated episodes of transient loading at the excavation site.

Jafari et al. (2002) proposed variation of the shear strength of rock joints due to cyclic loadings. Identical joint surfaces were prepared using a developed moulding method with special mortar and shear tests were performed on these samples under both static and cyclic loading conditions. Different levels of shear displacement were applied on the samples to study joint behaviour before and during considerable relative shear displacement. It was found that the shear strength of joints is related to rate of displacement (shearing velocity), number of loading cycles and stress amplitude. Finally, based on the experimental results, mathematical models were developed for evaluation of shear strength in cyclic loading conditions.

Jafari et al. (2004) evaluate the effects of small repetitive earthquakes on the strength parameters of rock joints in active seismic zones which is of interest of the designers of underground constructions. In order to evaluate these effects, it is necessary to study the behaviour of rock joints under dynamic and cyclic loadings. The results are presented as a systematic study on the behaviour of artificial rock joints subjected to cyclic shearing. More than 30 identical replicas have been tested using triaxial compression devices under different conditions of monotonic and cyclic loading. The surfaces of the tested rock joints are given regular triangular saw-tooth shapes with maximum inclination angle of (i-value) 15 degrees having small roughness on the surfaces of the teeth and other geometrical parameters of the joint surface and sample, as shown in Figure 2.4. At the first stage a few samples have been tested in monotonic loading modes under various confining pressures and rate of displacement. In the second series of tests, small cyclic loads were applied on the samples for increasing number of cycles, frequency levels and stress amplitudes. These were then followed by monotonic loading again. The variations of maximum and residual shear strengths for each test have been studied. The results show increase of shear strength as a result of the increase in confining pressure and they display decrease of shear strength due to the increase of rate of loading, number of cycles, frequency levels and stress amplitudes.

Grasselli and Egger (2003) represent a new constitutive criterion, relating stress and displacements, proposed to model the shear resistance of joints under constant normal load conditions. It is based on an empirical description of the surface, and on the results from more than 50 constant-normal-load direct-shear tests performed on replicas of tensile joints and on induced tensile fractures for seven rock types. This constitutive model is able to describe experimental shear tests conducted in the laboratory.

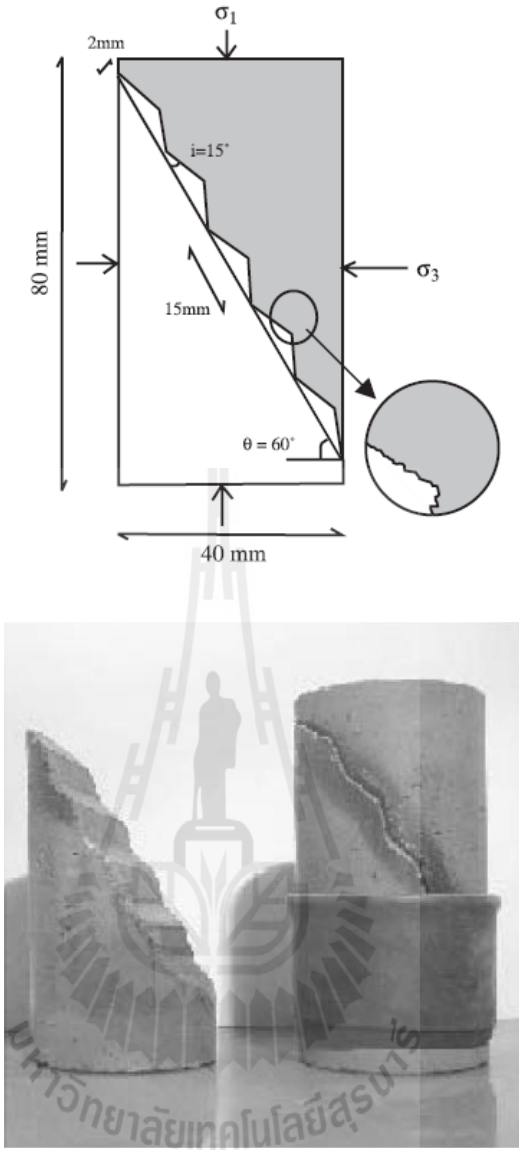

Figure 2.4 Schematic section and dimensions of the prepared saw-tooth sample (Jafari et al., 2004)

Moreover, the parameters required in the model can be easily measured through standard laboratory tests. The proposed criterion was also used to estimate the joint roughness coefficient (JRC) value. The predicting values were successfully correlated with JRC values obtained by back analysis of shear tests.

Puntel et al. (2006) formulate a generalized interface model for joints and cracks in quasi-brittle materials. The proposed model marries an existing fracture mechanics based one developed for monotonic loading of concrete with another frictional based model developed for the cyclic response of rock joints to address the (reverse) cyclic response of rough surfaces in the presence of cohesive stresses is correctly addressed. The properties of the model and its capability to capture several experimentally observed behaviors are shown by the numerical simulations performed. This joint constitutive model is particularly suitable to simulate the seismic response of dam/rock joints subjected to seismic excitation, or of concrete joints under reverse cyclic loading.

Jing et al. (1993) propose a conceptual model for the behaviour of rock joints during cyclic shear and under constant normal stresses according to results from shear tests with 50 concrete replicas of rock joints. The shear strength and deformability of joint samples were found to be both anisotropic and stress dependent. Based on these experimental results, a two-dimensional constitutive model was developed for rock joints undergoing monotonic or cyclic loading sequences. The joint model was formulated in the framework of non-associated plasticity, coupled with empirical relations representing the surface roughness degradation, appearance of peak and residual shear stresses, different rates of dilatancy and contraction, variable normal stiffness with normal deformation, and dependence of shear strength and deformability on the normal stress. The second law of thermodynamics was represented by an inequality and used to restrict the values of some of the material parameters in the joint model. The new joint model was implemented into a two-dimensional Distinct Element Method Code, UDEC, and its predictions agreed well with some well-known test results.

CHAPTER III

SAMPLE PREPARATION

3.1 Introduction

This chapter describes the rock sample preparation. The tested rocks are from three sources: Phu Phan sandstone, Saraburi limestone, and Saraburi granite (hereafter called PPSS, SLS and SGR). Sample preparation is carried out in the laboratory at the Suranaree University of Technology.

3.2 Sample preparation

Samples for shear strength of rock fractures under cyclic loading test are prepared to obtain rectangular blocks with nominal dimensions of 10×10×16 cm^3 (Table 3.1). Specimens with smooth surface are made by saw-cutting at the mid-section of the blocks. Some saw-cut surface specimens are shown in Figure 3.1. Specimens with rough surface are prepared by applying a line at the mid-section of the specimens until splitting tensile failure occurs (tension-induced fractures) (Figure 3.2). Some rough surface specimens are shown in Figure 3.3. For both smooth and rough fracture specimens, the upper block is trimmed out about 1 cm to obtain constant contact area during shearing. The tested fracture area is 8×10 cm^2. The asperity amplitudes on the fracture planes are measured from the laser-scanned profiles along the shear direction (Figures 3.4 through 3.6). The readings are made to the nearest 0.01 mm. The maximum amplitudes are used to estimate the joint roughness coefficients (JRC) of each fracture based on Barton's chart (Barton, 1982). Properties of the tested specimens are given in Table 3.2.

Table 3.1 Dimension of specimens.

Specimen no.	Width (cm)	Length (cm)	Height (cm)	Fracture area (cm^2)
Phu-Phan Sandstone -01	8.0	10.4	16.1	82.84
Phu-Phan Sandstone -02	8.2	10.6	16.1	86.71
Phu-Phan Sandstone -03	8.0	10.2	16.0	81.35
Phu-Phan Sandstone -04	8.0	10.5	16.0	83.94
Phu-Phan Sandstone -05	8.1	10.2	15.9	82.58
Phu-Phan Sandstone -06	8.2	10.3	15.9	84.4
Saraburi Granite -01	7.9	10.0	16.0	79.03
Saraburi Granite -02	8.1	10.3	16.0	83.42
Saraburi Granite -03	8.2	10.7	15.9	87.95
Saraburi Granite -04	7.9	9.9	15.8	78.39
Saraburi Granite -05	8.0	10.2	15.8	81.74
Saraburi Granite -06	8.1	10.2	15.8	82.32
Saraburi Limestone -01	7.8	9.9	16.1	77.55
Saraburi Limestone -02	8.3	10.5	15.8	87.10
Saraburi Limestone -03	8.0	10.2	15.9	81.87
Saraburi Limestone -04	8.1	10.6	16.0	85.81
Saraburi Limestone -05	8.2	10.5	15.9	86.45
Saraburi Limestone -06	8.1	10.6	15.9	85.55

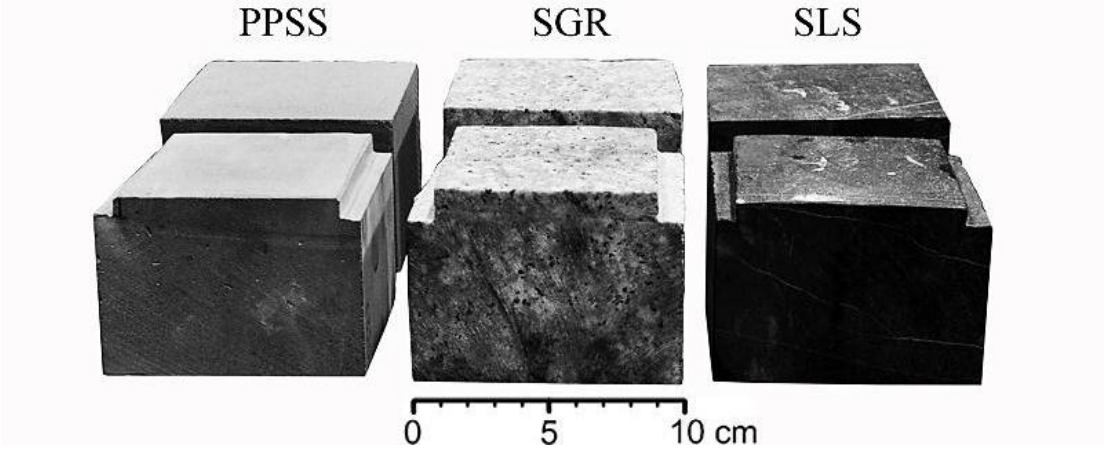

Figure 3.1 Some rock specimens with smooth saw-cut surfaces.

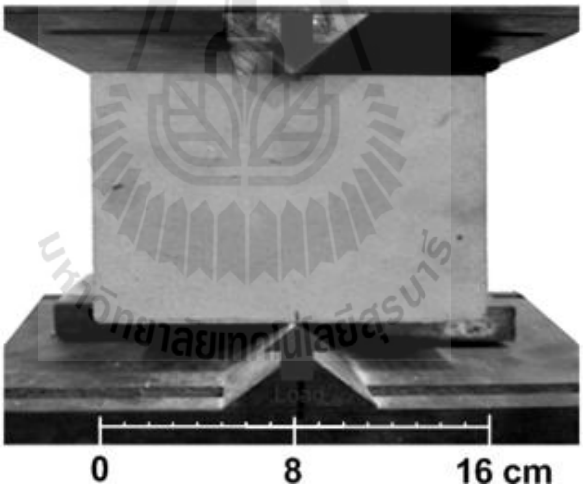

Figure 3.2 Splitting method by line loading to obtain tensile fractures of PPSS specimens prepared for cyclic loading testing.

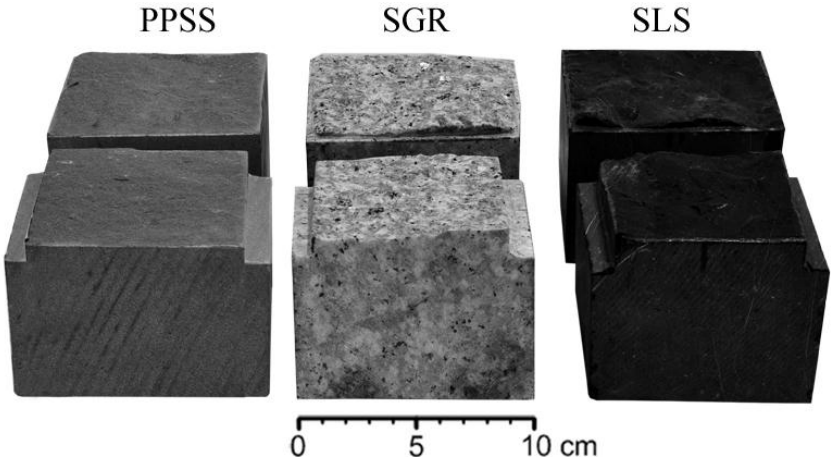

Figure 3.3 Some rock specimens with tension-induced fractures.

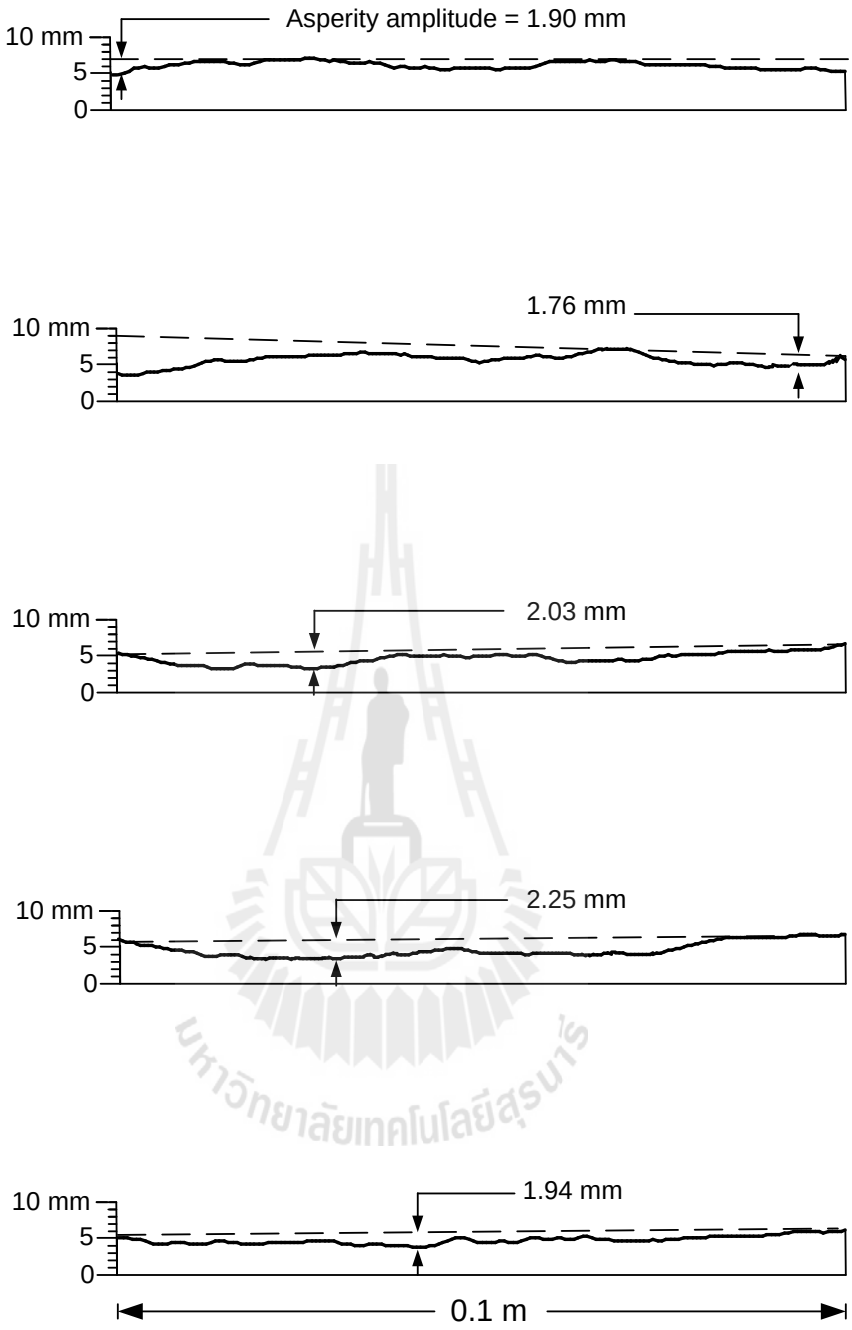

Figure 3.4 Laser-scanned profiles of tension-induced fracture from Phu Phan sandstone.

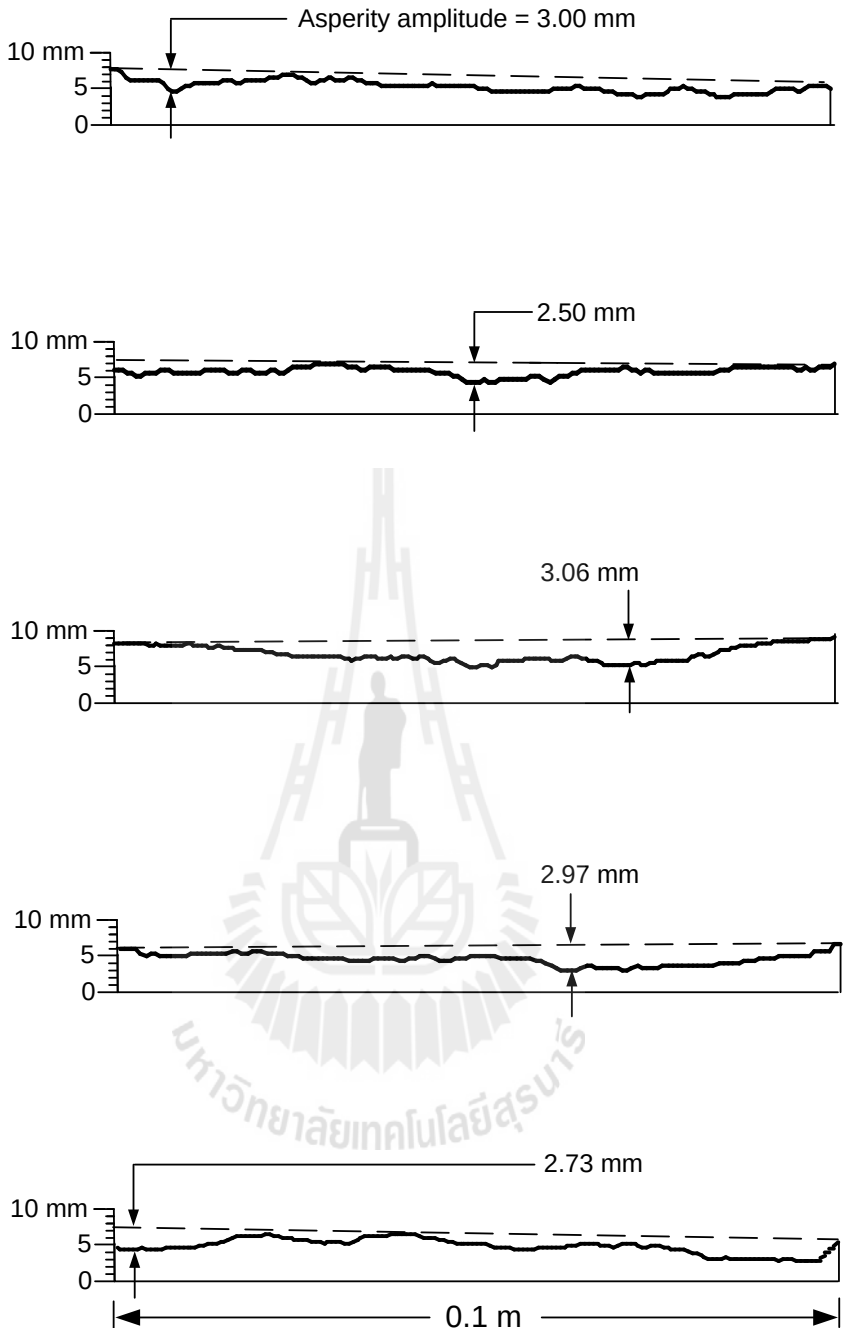

Figure 3.5 Laser-scanned profiles of tension-induced fracture from Saraburi granite.

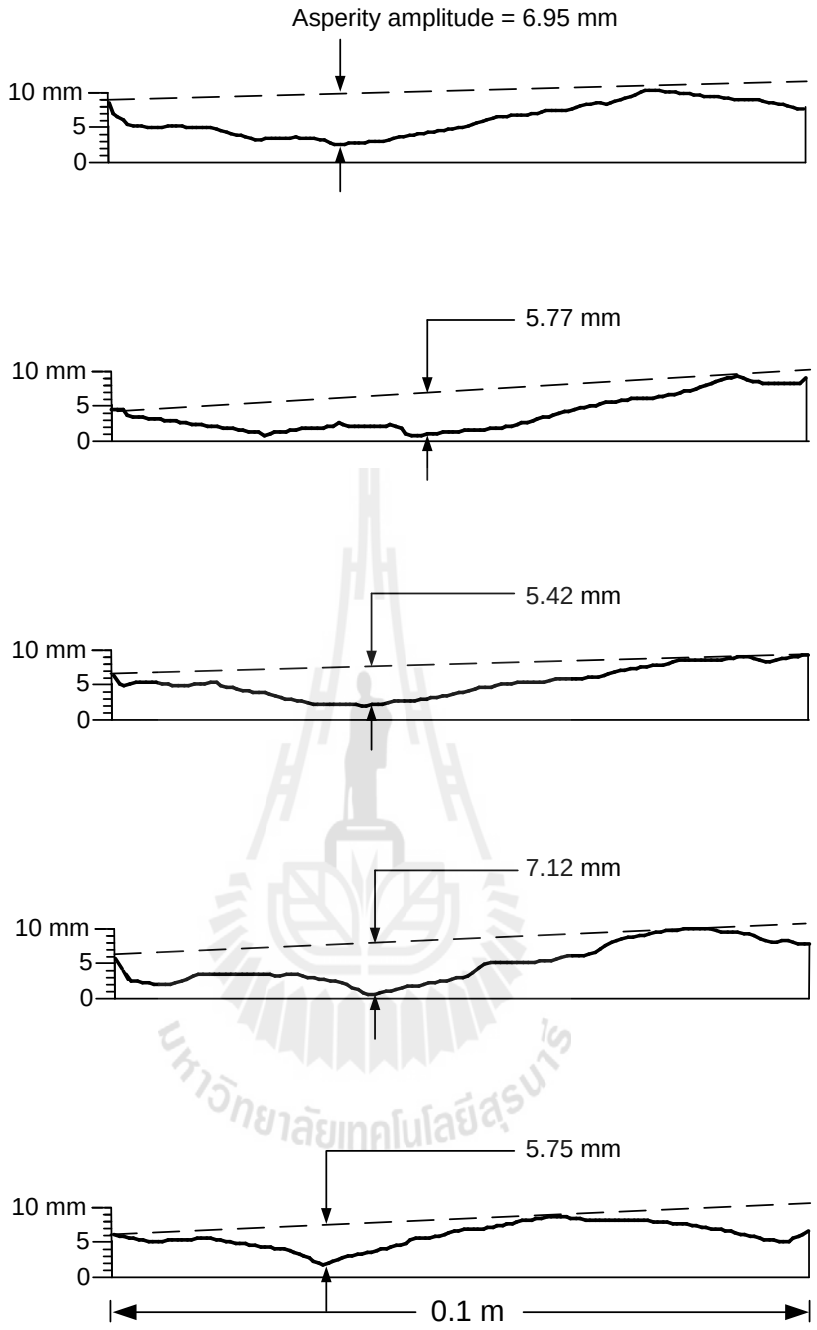

Figure 3.6 Laser-scanned profiles of tension-induced fracture from Saraburi limestone.

Table 3.2 Properties of specimens.

Specimen No.	Dry density (g/cc)	JRC	Normal stress (MPa)
Phu-Phan Sandstone -01	2.21	8	0.5
Phu-Phan Sandstone -02	2.31	7	1.0
Phu-Phan Sandstone -03	2.33	8	2.0
Phu-Phan Sandstone -04	2.30	9	3.0
Phu-Phan Sandstone -05	2.26	8	4.0
Phu-Phan Sandstone -06	2.27	smooth surface	0.5, 1, 2, 3, and 4
Saraburi Granite -01	2.66	12	0.5
Saraburi Granite -02	2.70	10	1.0
Saraburi Granite -03	2.71	12	2.0
Saraburi Granite -04	2.71	12	3.0
Saraburi Granite -05	2.68	11	4.0
Saraburi Granite -06	2.71	smooth surface	0.5, 1, 2, 3, and 4
Saraburi Limestone -01	2.83	20	0.5
Saraburi Limestone -02	2.82	20	1.0
Saraburi Limestone -03	2.85	20	2.0
Saraburi Limestone -04	2.83	20	3.0
Saraburi Limestone -05	2.87	20	4.0
Saraburi Limestone -06	2.80	smooth surface	0.5, 1, 2, 3, and 4

CHAPTER IV

LABORATORY TESTING

4.1 Introduction

The objective of the laboratory testing is to determine the shear strength on smooth saw-cut surface and tension-induced fractures of the three rock types. This chapter describes the test method and test results. The changes of the displacement and dilation, and the applied shear stresses are monitored and used to calculate the changes of the shear strength and dilation rates as a function of loading cycle.

4.2 Test method

The test method and calculation follow as much as practical the ASTM (D5607-08) standard practice. Each specimen is sheared once under each normal stress using a direct shear device (SBEL DR44, capacity of 10,000 pounds normal load and 30,000 pounds shear force) (Figure 4.1). The specimen is placed in direct shear load frame which is used to applied normal stresses of 0.5, 1, 2, 3, and 4 MPa. The rates of shear displacement are 0.01–0.02 mm/s. The number of loading cycles is 10 with the maximum shear displacement of ±5 mm. The applied normal and shear forces and the corresponding normal and shear displacements are monitored and recorded. Linear variable differential transformers (LVDT's) are used to measure the shear and normal displacements. Each shear loading cycle is divided into four stages: forward advance (stage I) when the specimen moves from the origin to +5 mm with

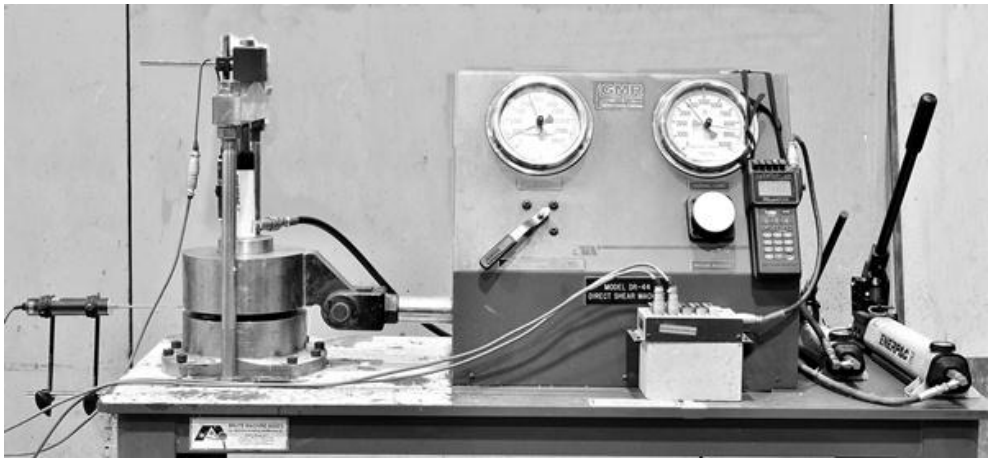

Figure 4.1 Direct shear device SBEL DR44 used in this study.

positive corresponding shear stress; forward return (stage II) when the specimen returns from +5 to the origin with negative shear stress; backward advance (stage III) when the specimen moves from the origin to -5 mm with negative corresponding shear stress; backward return (stage IV) when the specimen returns from -5 to the origin with positive shear stress (Figure 4.2). As expected, the greater the normal stress applied, the greater the peak shear stress obtained. The peak shear stress is calculated and plotted against the corresponding normal stress. The peak shear strength (τ_p) and residual shear strength (τ_r) are calculated by the equations (Hibbeler, 2011);

$$\tau_p = P_p / A \tag{4.1}$$

$$\tau_r = P_r / A \tag{4.2}$$

where P_p is the maximum shear force, P_r is the residual shear force, and A is the contact area between both specimens. Tables 4.1 through 4.6 lists the peak shear stresses calculated for 10 cycles of three rock types.

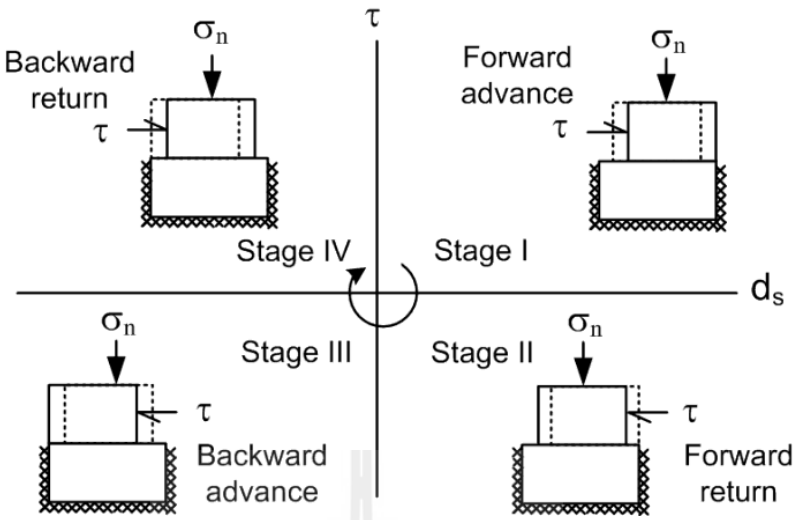

Figure 4.2 Shearing paths for four stages in one cycle.

Table 4.1 Shear strengths of the PPSS with tension-induced fractures.

		Normal stress (MPa)				
		0.5	1	2	3	4
		Peak shear strength (MPa)				
Cycle No.	C1	1.02	1.54	2.95	4.29	5.12
	C2	0.67	1.08	1.97	2.65	3.34
	C3	0.67	1.03	1.97	2.65	3.23
	C4	0.67	1.03	1.97	2.60	3.23
	C5	0.64	1.03	1.97	2.65	3.23
	C6	0.64	1.03	1.97	2.65	3.23
	C7	0.64	1.03	1.97	2.65	3.23
	C8	0.64	1.08	1.97	2.65	3.23
	C9	0.64	1.03	1.97	2.65	3.23
	C10	0.64	1.03	1.97	2.65	3.23

Table 4.2 Shear strengths of the SGR with tension-induced fractures.

		Normal stress (MPa)				
		0.5	1	2	3	4
		Peak shear strength (MPa)				
Cycle No.	C1	1.80	2.77	4.55	5.45	6.04
	C2	0.73	1.33	2.23	2.78	3.81
	C3	0.73	1.28	2.23	2.78	3.70
	C4	0.73	1.23	2.23	2.78	3.81
	C5	0.73	1.28	2.23	2.84	3.81
	C6	0.73	1.23	2.23	2.84	3.81
	C7	0.73	1.28	2.23	2.95	3.81
	C8	0.73	1.23	2.23	2.95	3.81
	C9	0.73	1.28	2.23	2.95	3.81
	C10	0.73	1.28	2.23	2.95	3.92

Table 4.3 Shear strengths of the SLS with tension-induced fractures.

		Normal stress (MPa)				
		0.5	1	2	3	4
		Peak shear strength (MPa)				
Cycle No.	C1	1.15	2.15	3.21	4.45	5.46
	C2	0.75	1.33	1.85	2.90	3.65
	C3	0.75	0.97	1.96	2.69	3.60
	C4	0.69	1.23	2.07	2.59	3.65
	C5	0.69	1.23	2.07	2.79	3.71
	C6	0.75	1.12	2.17	2.85	3.71
	C7	0.75	1.33	2.17	2.69	3.60
	C8	0.69	1.33	2.17	2.54	3.71
	C9	0.69	1.23	2.23	2.69	3.65
	C10	0.69	1.33	2.17	2.69	3.71

Table 4.4 Shear strengths of the PPSS with smooth saw-cut surfaces.

		Normal stress (MPa)				
		0.5	1	2	3	4
		Peak shear strength (MPa)				
Cycle No.	C1	0.42	0.63	1.16	1.74	2.53
	C2	0.42	0.63	1.16	1.79	2.53
	C3	0.42	0.63	1.16	1.79	2.53
	C4	0.42	0.63	1.16	1.79	2.53
	C5	0.42	0.63	1.16	1.79	2.53
	C6	0.42	0.63	1.16	1.79	2.53
	C7	0.42	0.63	1.16	1.79	2.53
	C8	0.42	0.63	1.16	1.79	2.53
	C9	0.42	0.63	1.16	1.79	2.53
	C10	0.42	0.63	1.16	1.79	2.53

Table 4.5 Shear strengths of the SGR with smooth saw-cut surfaces.

		Normal stress (MPa)				
		0.5	1	2	3	4
		Peak shear strength (MPa)				
Cycle No.	C1	0.49	0.81	1.62	2.27	2.92
	C2	0.49	0.81	1.62	2.27	2.97
	C3	0.49	0.81	1.62	2.27	2.97
	C4	0.49	0.81	1.62	2.27	2.97
	C5	0.49	0.81	1.62	2.27	2.97
	C6	0.49	0.81	1.62	2.27	2.97
	C7	0.49	0.81	1.62	2.27	2.97
	C8	0.49	0.81	1.62	2.27	2.97
	C9	0.49	0.81	1.62	2.27	2.97
	C10	0.49	0.81	1.62	2.27	2.97

Table 4.6 Shear strengths of the SLS with smooth saw-cut surfaces.

		Normal stress (MPa)				
		0.5	1	2	3	4
		Peak shear strength (MPa)				
Cycle No.	C1	0.47	0.73	1.25	1.56	2.50
	C2	0.47	0.73	1.25	1.56	2.50
	C3	0.47	0.73	1.25	1.56	2.50
	C4	0.47	0.73	1.25	1.56	2.50
	C5	0.47	0.73	1.25	1.56	2.50
	C6	0.47	0.73	1.25	1.56	2.50
	C7	0.47	0.73	1.25	1.56	2.50
	C8	0.47	0.73	1.25	1.56	2.50
	C9	0.47	0.73	1.25	1.56	2.50
	C10	0.47	0.73	1.25	1.56	2.50

4.3 Test results

4.3.1 Tension-induced fractures

The results are presented in terms of the shear stresses as a function of shear displacement under constant normal stresses at 0.5, 1, 2, 3, and 4 MPa. Figures 4.3 through 4.5 show the shear stress-displacement curves under 0.5, 1, 2, 3, and 4 MPa normal stresses. Shear stress and displacement curves of the first cycle reveal the peak shear stress and residual shear stress. In the second to tenth cycle of shear loading, the peak shear stress disappears and gradually reduces to the level of residual shear stress. Figures 4.6 through 4.8 shows the dilation as a function of shear displacement on tension-induced fractures under 0.5, 1, 2, 3, and 4 MPa normal stresses. The cyclic loading has a significant effect on dilation rate and degradation of asperities; that is, the dilation rates of the second to tenth cycle are less than that of the first one for all rock types.

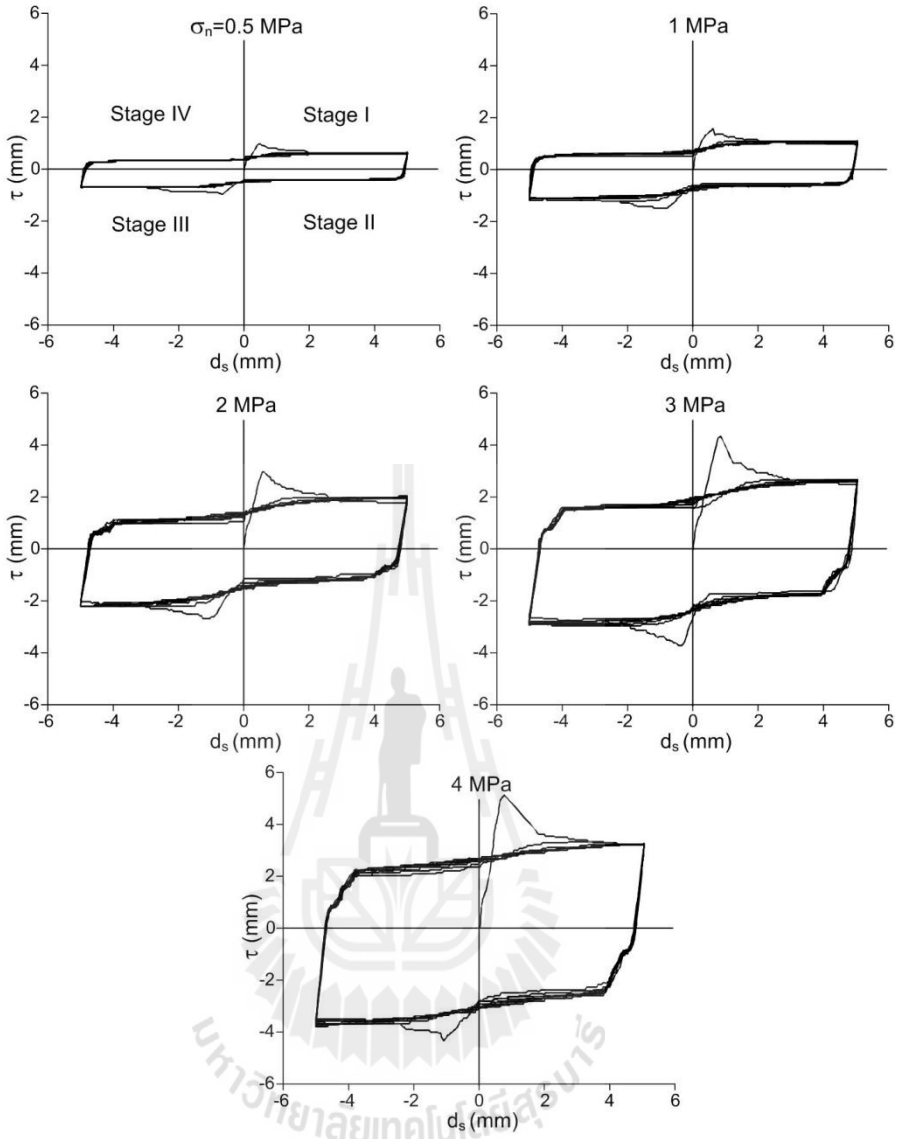

Figure 4.3 Cyclic shear stresses of tension-induced fracture specimens as a function of shear displacement under normal stresses of 0.5, 1, 2, 3, and 4 MPa for PPSS.

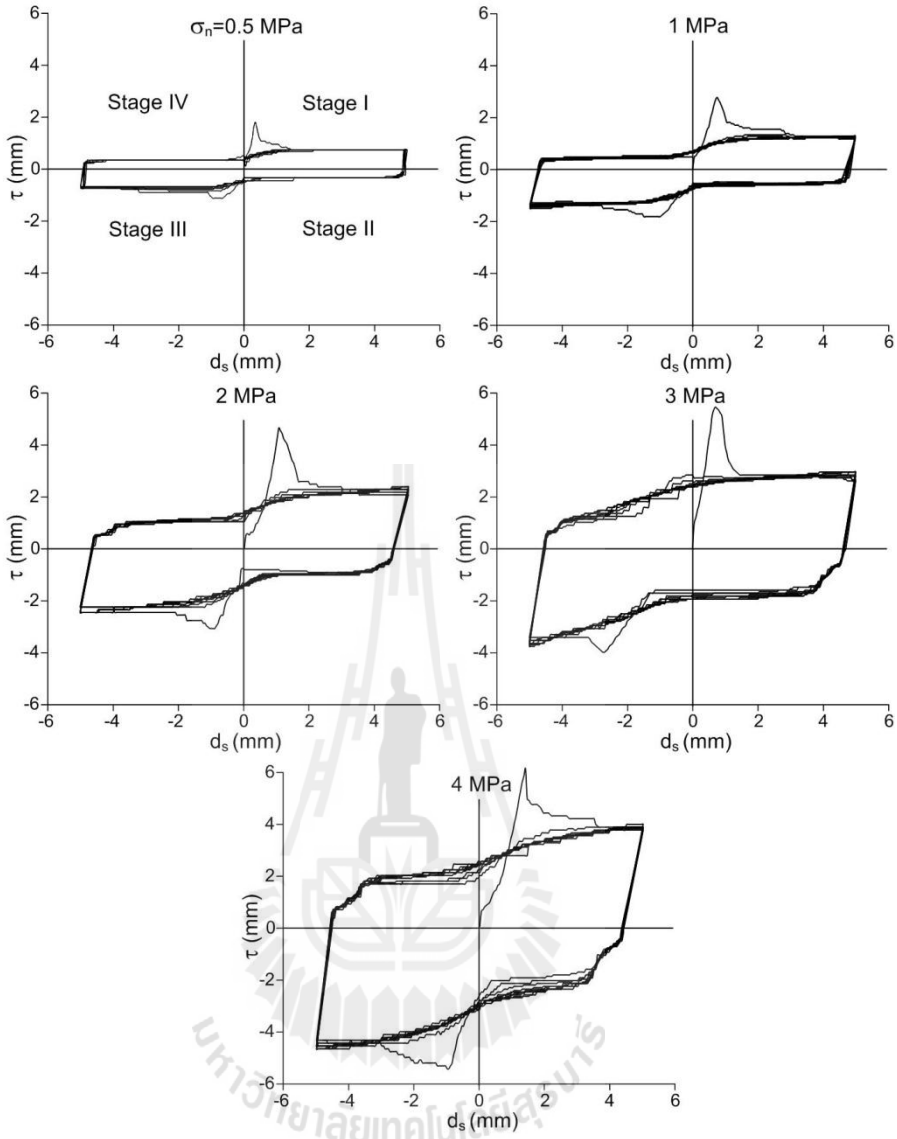

Figure 4.4 Cyclic shear stresses of tension-induced fracture specimens as a function of shear displacement under normal stresses of 0.5, 1, 2, 3, and 4 MPa for SGR.

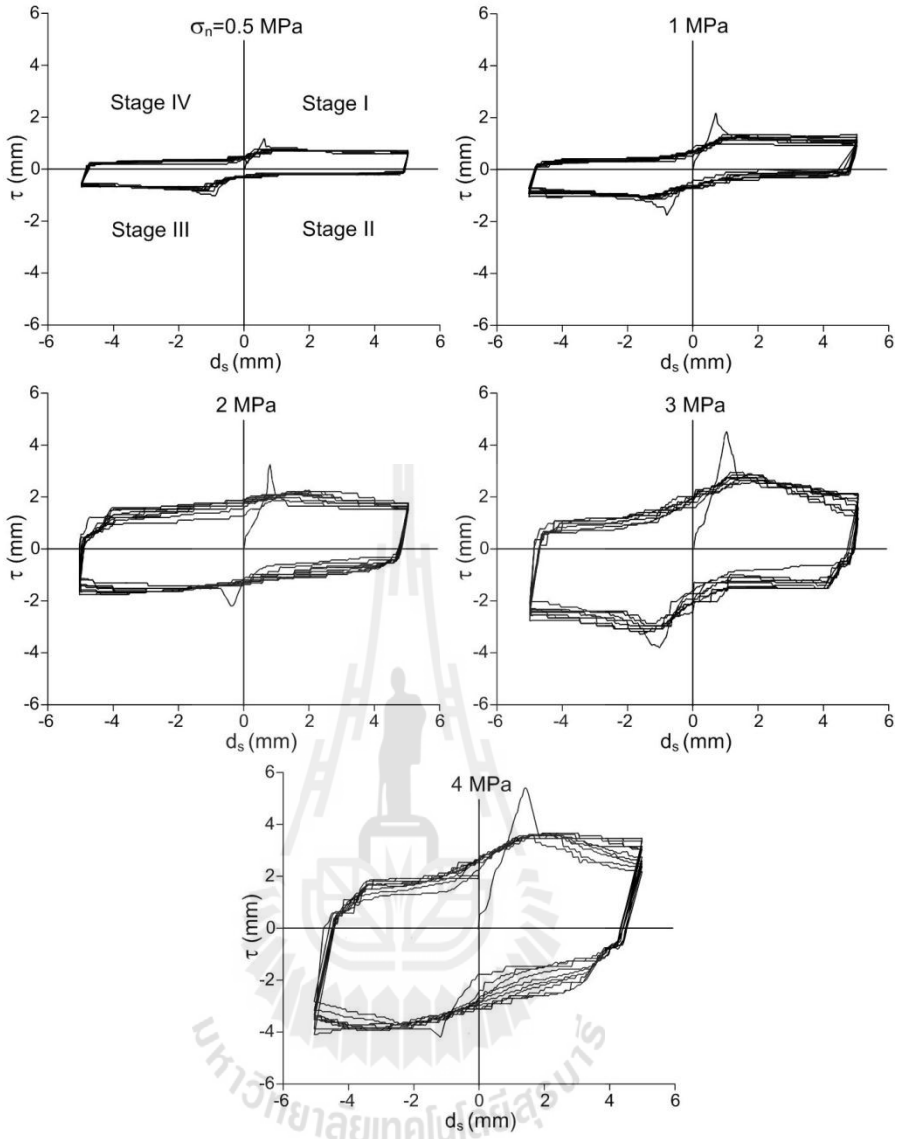

Figure 4.5 Cyclic shear stresses of tension-induced fracture specimens as a function of shear displacement under normal stresses of 0.5, 1, 2, 3, and 4 MPa for SLS.

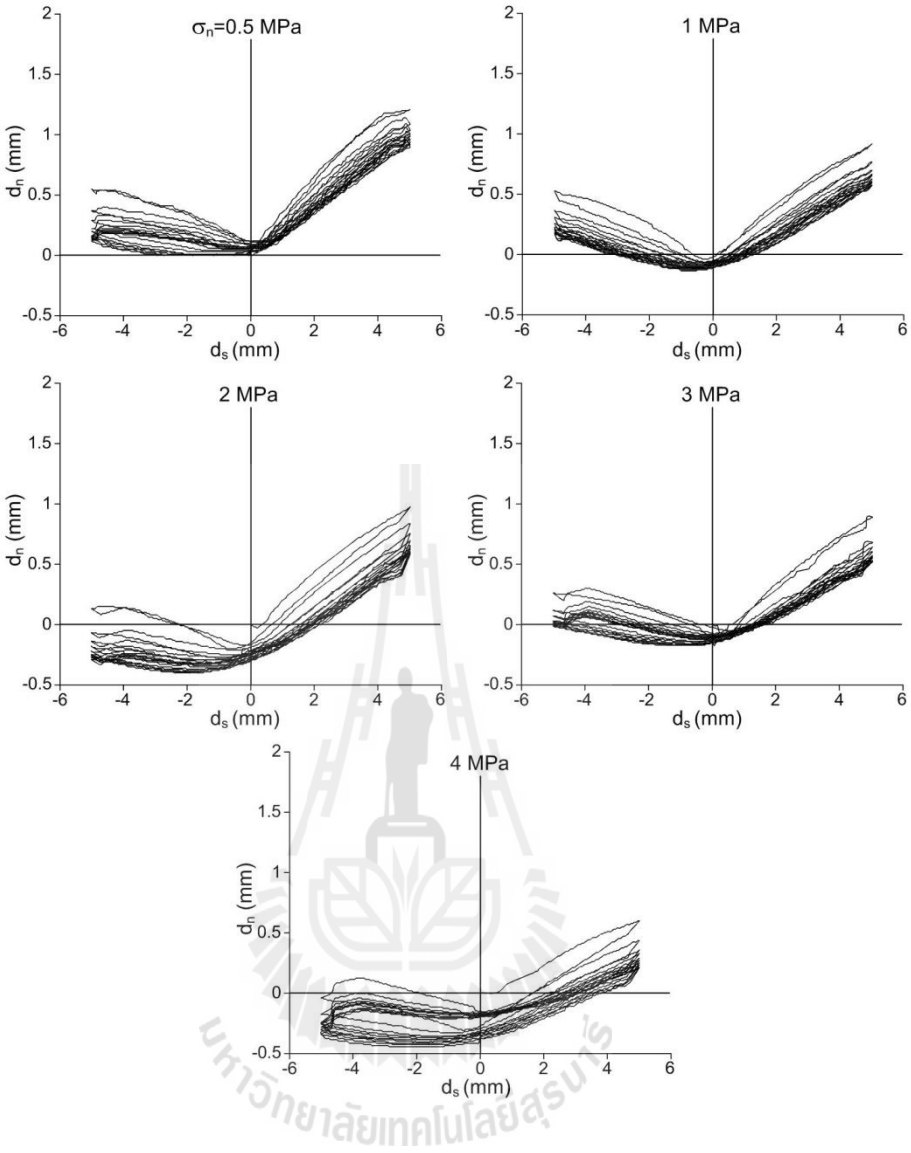

Figure 4.6 Normal displacement of tension-induced fracture specimens as a function of shear displacement under normal stresses of 0.5, 1, 2, 3, and 4 MPa for PPSS.

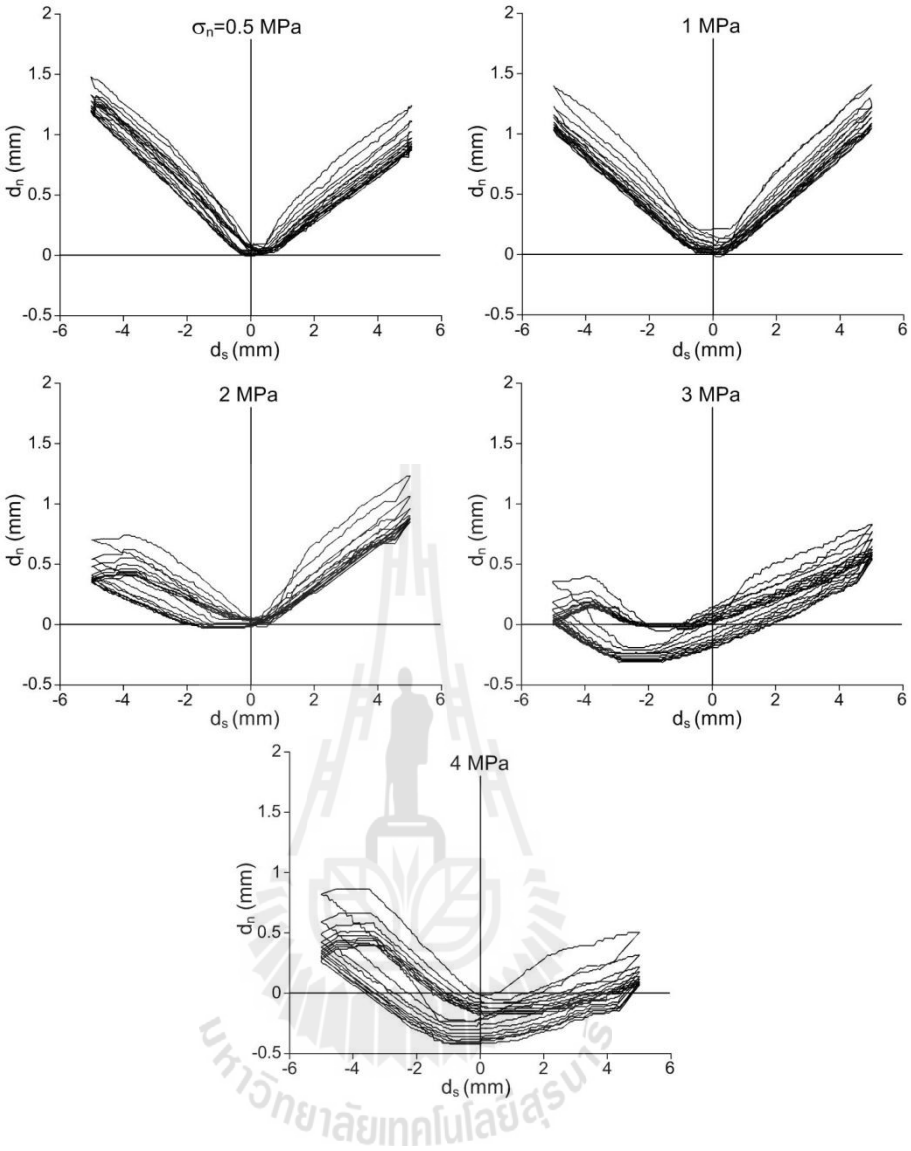

Figure 4.7 Normal displacement of tension-induced fracture specimens as a function of shear displacement under normal stresses of 0.5, 1, 2, 3, and 4 MPa for SGR.

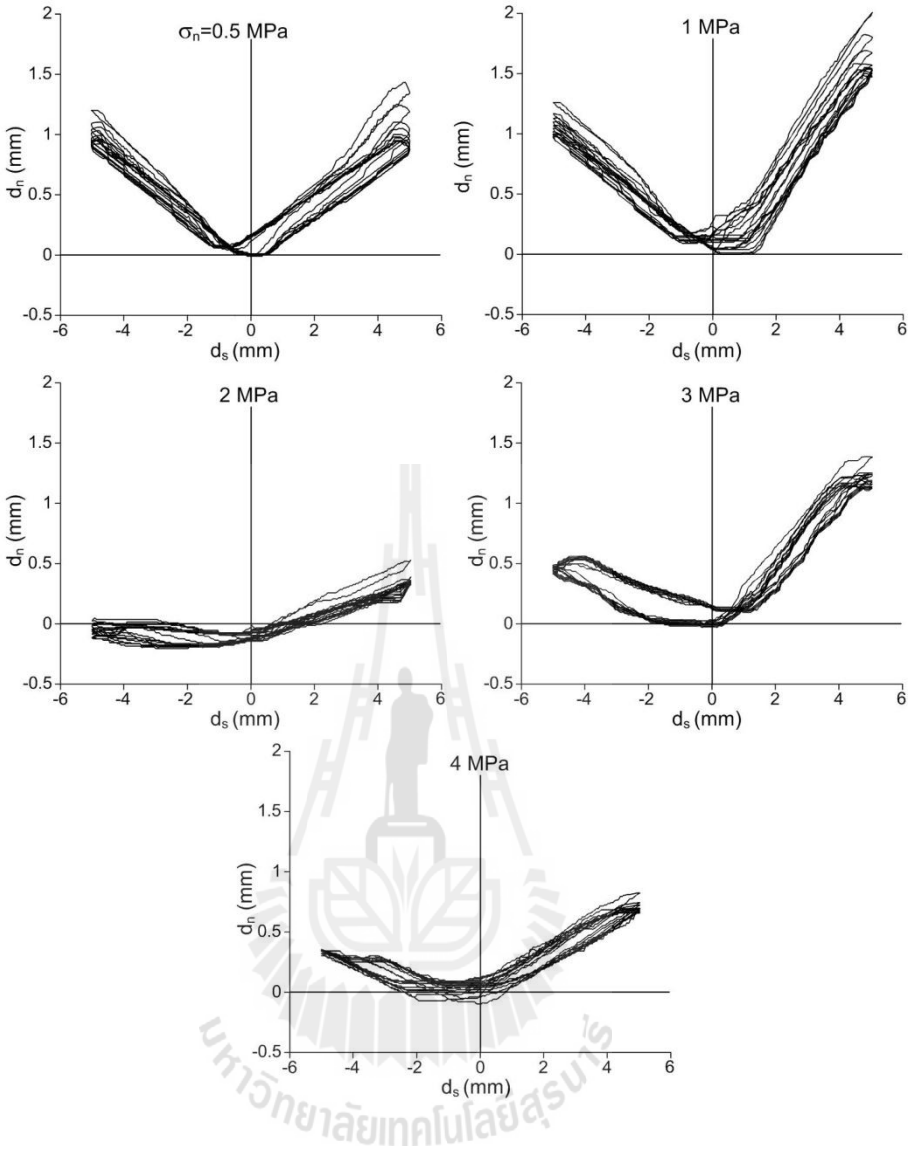

Figure 4.8 Normal displacement of tension-induced fracture specimens as a function of shear displacement under normal stresses of 0.5, 1, 2, 3, and 4 MPa for SLS.

4.3.2 Smooth saw-cut surfaces

Figures 4.9 through 4.11 show the shear stress-displacement curves under 0.5, 1, 2, 3, and 4 MPa normal stresses. No peak shear stress is detected for all normal loads and loading cycles. The results from cycle one to cycle ten are virtually identical. Figures 4.12 through 4.14 shows the dilation as a function of shear displacement on smooth saw-cut-surface specimens under 0.5, 1, 2, 3, and 4 MPa normal stresses. The results indicate that the dilation curves are also similar for all cycles. The shear strengths and dilation rates of the smooth fracture tend to be independent of the cyclic shearing.

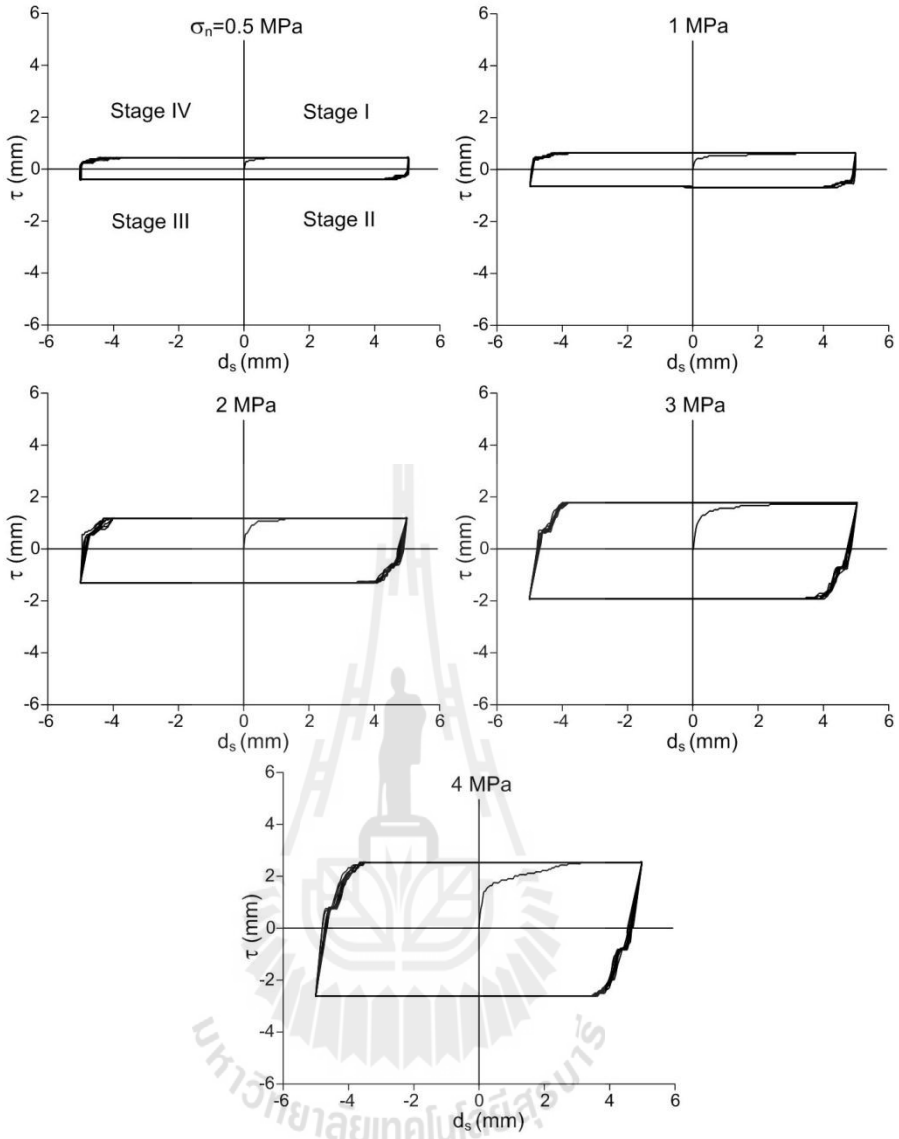

Figure 4.9 Cyclic shear stresses of smooth saw-cut surface specimens as a function of shear displacement under normal stresses of 0.5, 1, 2, 3, and 4 MPa for PPSS.

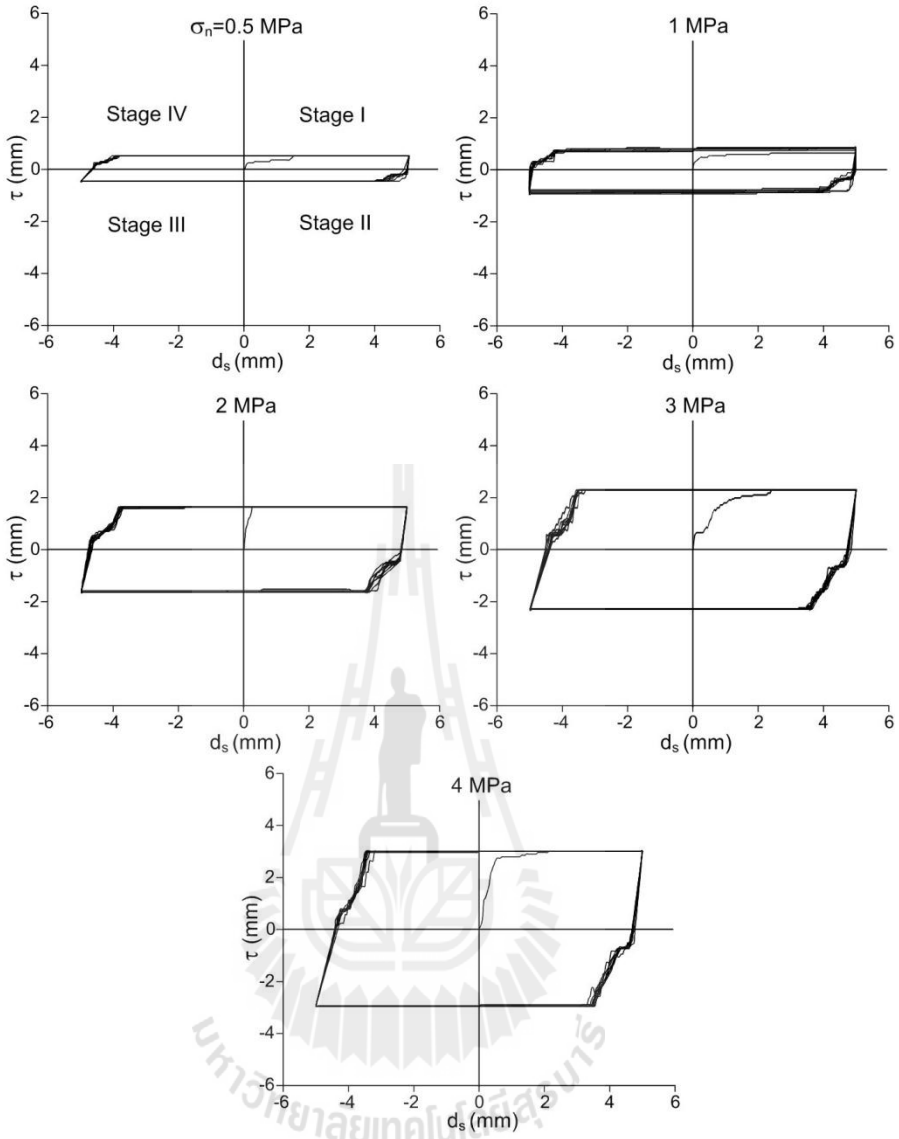

Figure 4.10 Cyclic shear stresses of smooth saw-cut surface specimens as a function of shear displacement under normal stresses of 0.5, 1, 2, 3, and 4 MPa for SGR.

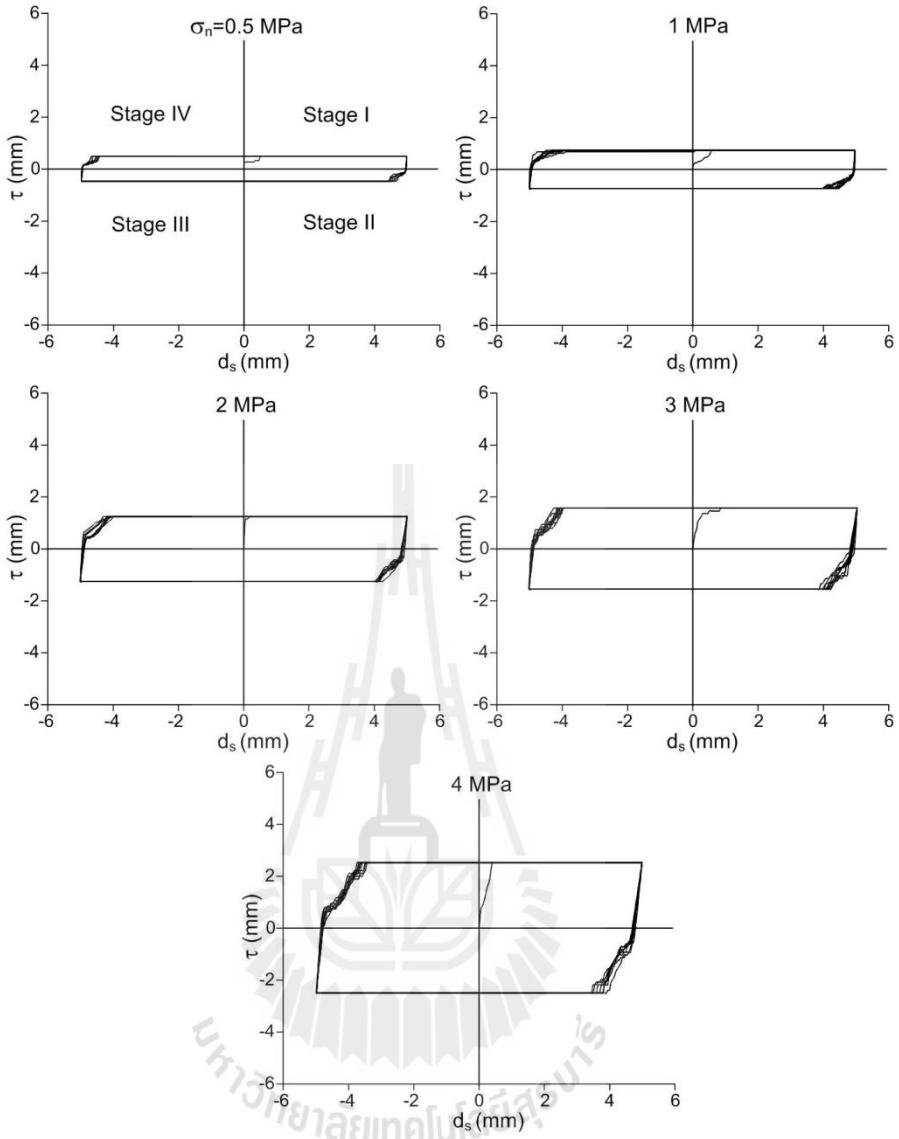

Figure 4.11 Cyclic shear stresses of smooth saw-cut surface specimens as a function of shear displacement under normal stresses of 0.5, 1, 2, 3, and 4 MPa for SLS.

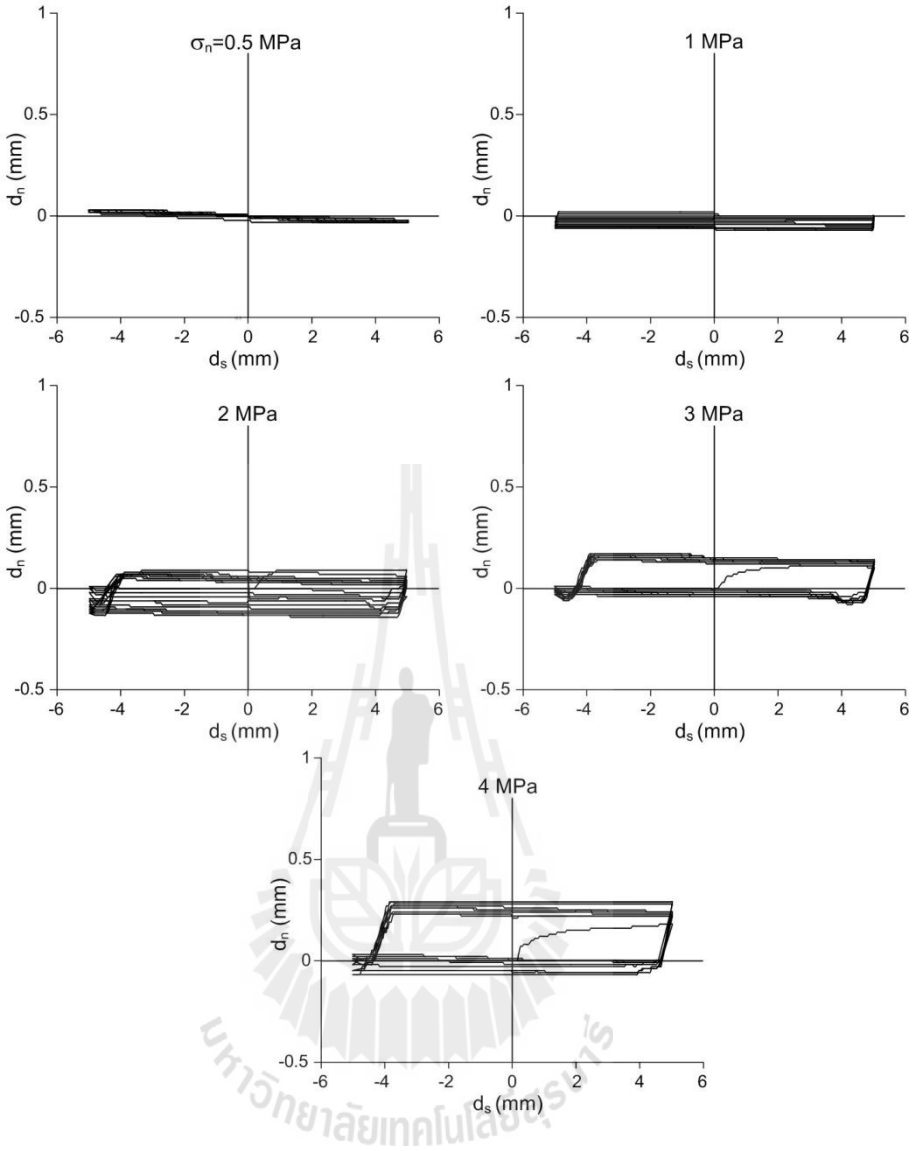

Figure 4.12 Normal displacement of smooth saw-cut surface specimens as a function of shear displacement under normal stresses of 0.5, 1, 2, 3, and 4 MPa for PPSS.

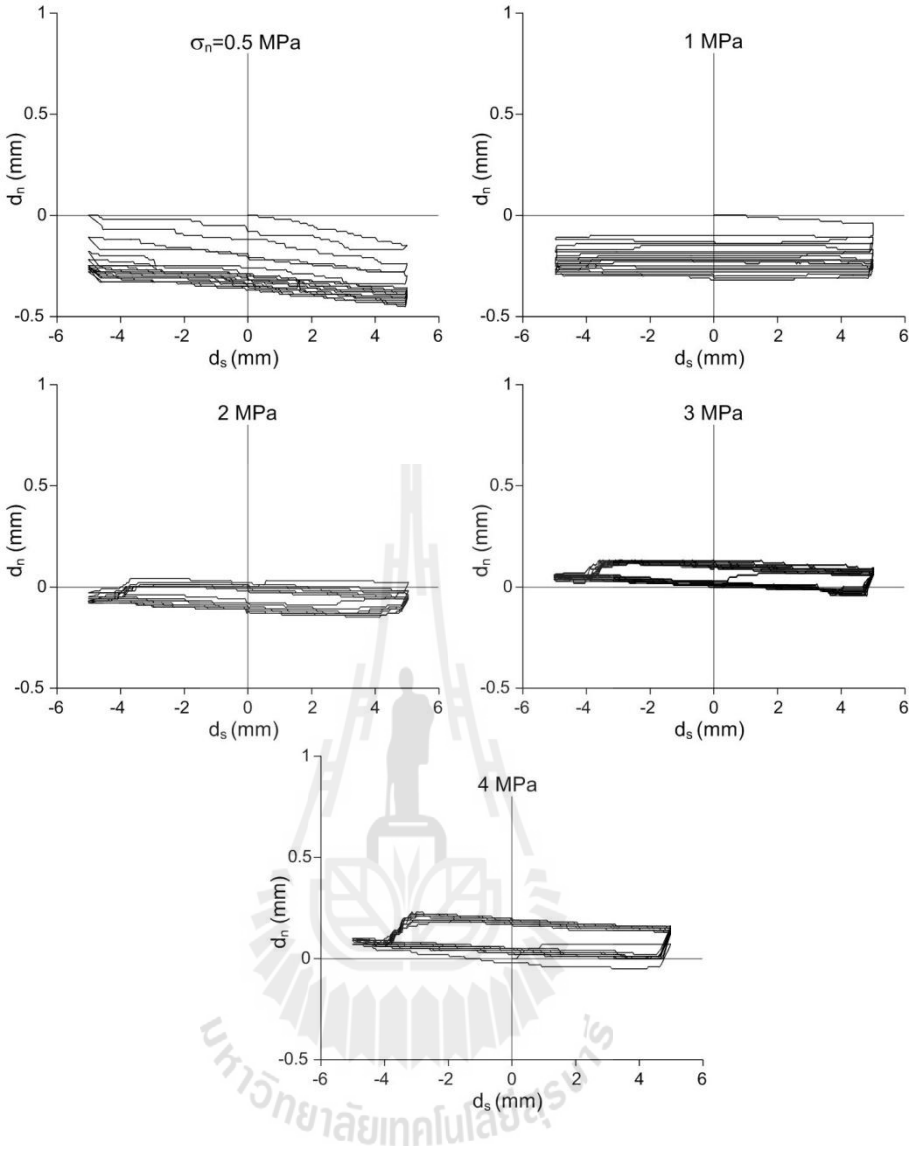

Figure 4.13 Normal displacement of smooth saw-cut surface specimens as a function of shear displacement under normal stresses of 0.5, 1, 2, 3, and 4 MPa for SGR.

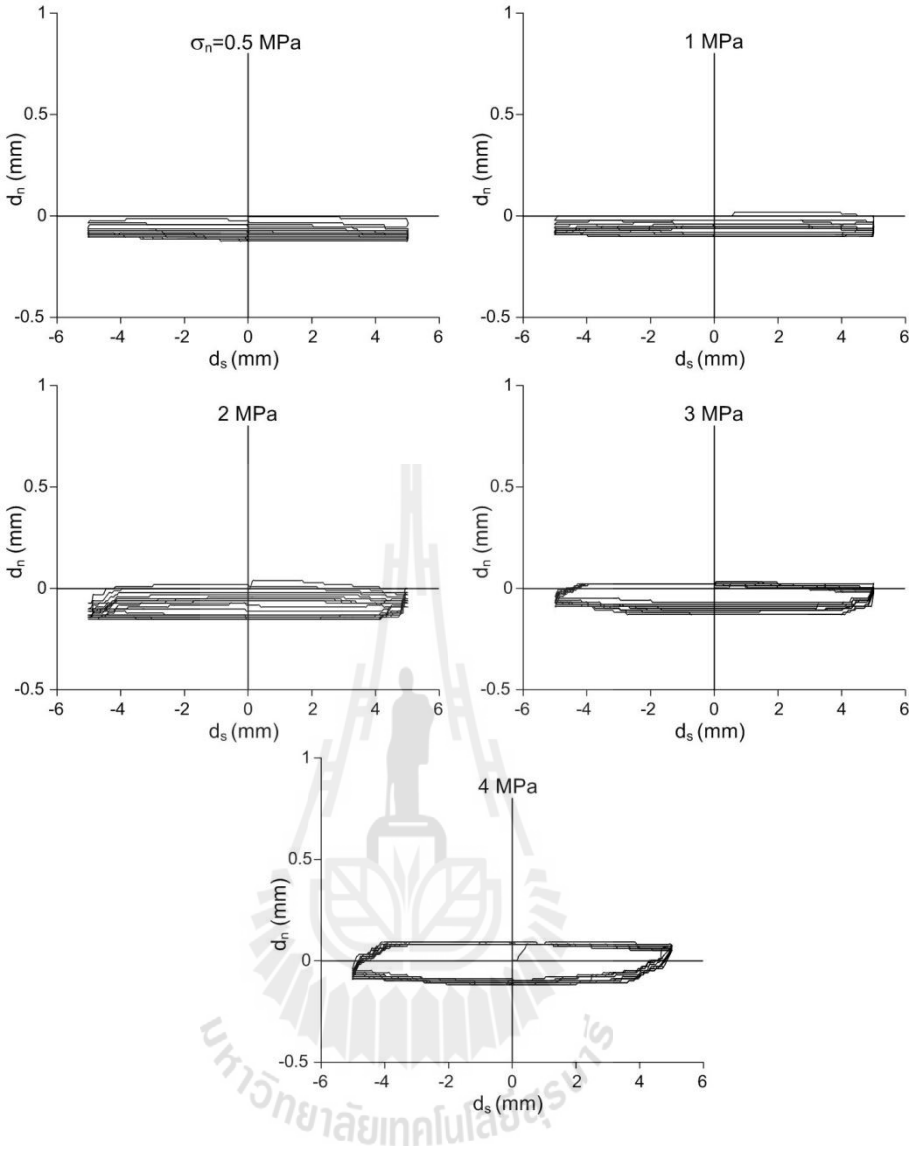

Figure 4.14 Normal displacement of smooth saw-cut surface specimens as a function of shear displacement under normal stresses of 0.5, 1, 2, 3, and 4 MPa for SLS.

CHAPTER V

MATHEMATICAL RELATIONSHIPS

5.1 Introduction

This chapter describes the mathematical relationships between the joint normal stiffness, joint shear stiffness, shear strength (cohesion and friction angle), dilation rate, with loading cycles under normal stresses at 0.5, 1, 2, 3 and 4 MPa.

5.2 Normal and shear stiffness of rock samples

Figure 5.1 shows the joint normal stiffness (K_n) as a function of normal stress. The increase of joint normal stiffness with normal stress is non-linear which can be represented by:

$$K_n = \omega \cdot \exp(\kappa \cdot \sigma_n) \quad (5.1)$$

where σ_n is the normal stress and parameters ω and κ are empirical constants (Table 5.1). From the equation (5.1), K_n can be calculated for each rock type as:

for PPSS;

$$K_n = 0.379 \cdot \exp(1.257 \cdot \sigma_n) \quad (5.2)$$

for SGR;

$$K_n = 0.424 \cdot \exp(1.021 \cdot \sigma_n) \quad (5.3)$$

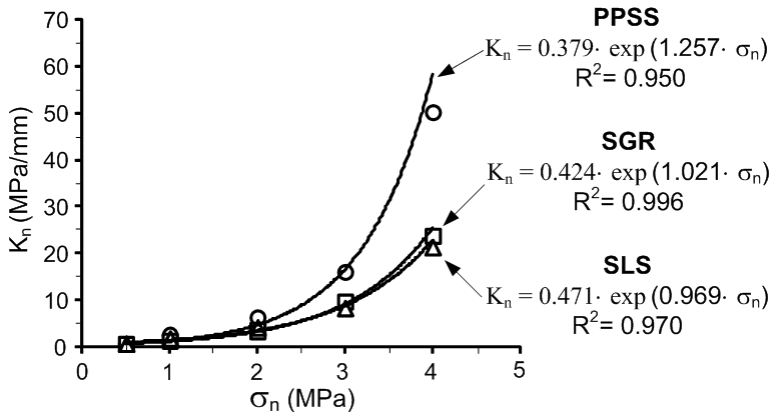

Figure 5.1 Joint normal stiffness as a function of normal stress.

Table 5.1 Summary of empirical constants ω and κ.

Rock type	ω (1/mm)	κ
PPSS	0.379	1.257
SGR	0.424	1.021
SLS	0.471	0.969

for SLS;

$$K_n = 0.471 \cdot \exp(0.969 \cdot \sigma_n) \quad (5.4)$$

Figure 5.2 plots the joint shear stiffness (K_s) as a function of the loading cycle at 0.5, 1, 2, 3, and 4 MPa normal stresses. It is calculated from the linear slope of the shear stress-displacement curves. Results for all rock types indicate that the increase of loading cycle can notably decrease the joint shear stiffness. The shear stiffness tends to increase with the normal stresses which agree with test results obtained by Jing et al (1993).

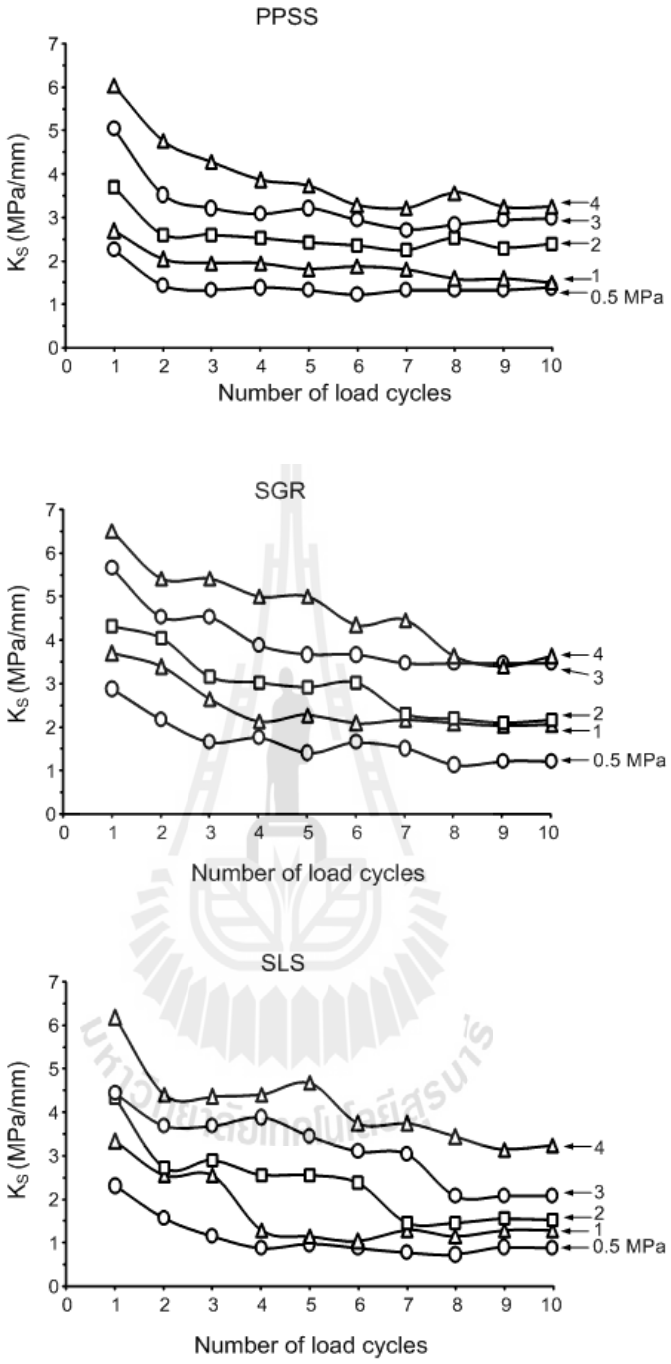

Figure 5.2 Joint shear stiffness as a function of number of loading cycles.

5.3 Shear strength as a function of loading cycles

Figure 5.3 shows the shear strengths of the tension-induced fractures as a function of normal stress for 10 cycles. According to the Coulomb criterion, the shear strength (τ) can be represented by (Jaeger et al., 2007) :

$$\tau_p = c + \sigma_n \tan \phi_p \quad (5.5)$$

$$\tau_r = c + \sigma_n \tan \phi_r \quad (5.6)$$

where σ_n is the normal stress, τ_p is peak shear strength, τ_r is residual shear strength, c is the cohesion, ϕ_p is peak friction angle and ϕ_r is residual friction angle and. The test results of tension-induced fractures well fit to the Coulomb criterion which can be represented by:

for PPSS;

$$\tau_p = 0.43 + \sigma_n \tan 51° \quad \text{MPa} \quad (5.7)$$

$$\tau_r = 0.34 + \sigma_n \tan 37° \quad \text{MPa} \quad (5.8)$$

for SGR;

$$\tau_p = 1.56 + \sigma_n \tan 51° \quad \text{MPa} \quad (5.9)$$

$$\tau_r = 0.38 + \sigma_n \tan 41° \quad \text{MPa} \quad (5.10)$$

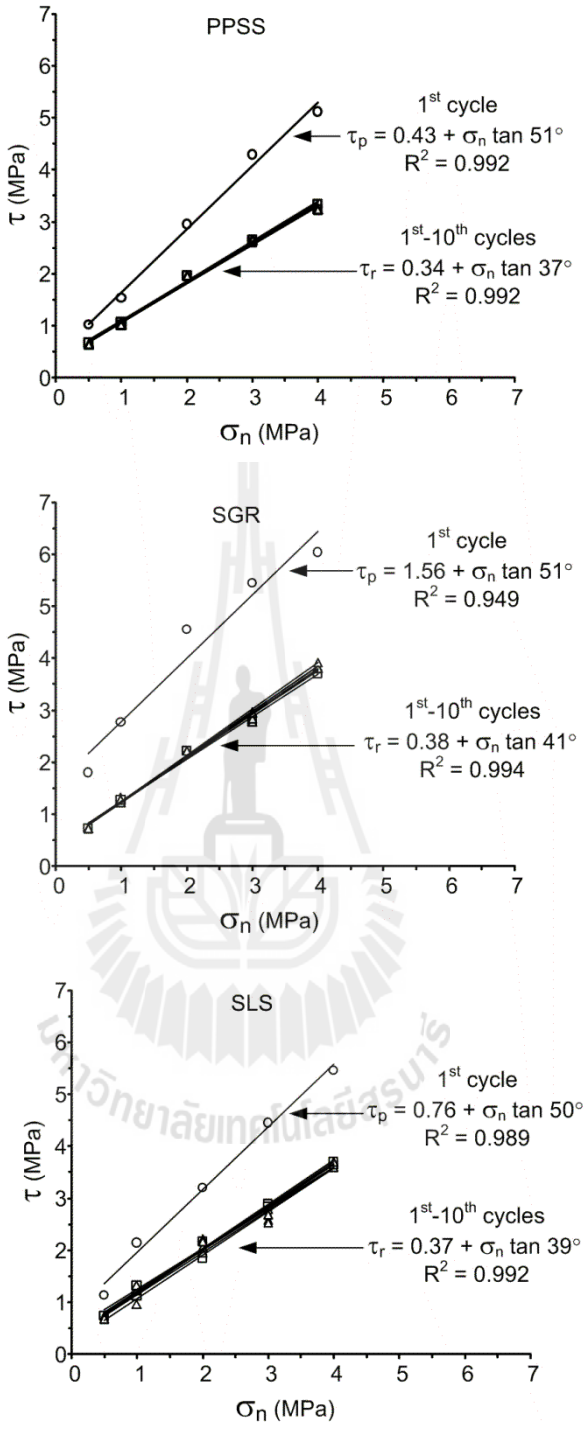

Figure 5.3 Shear strength as a function of normal stress for tension-induced fractures.

for SLS;

$$\tau_p = 0.76 + \sigma_n \tan 50° \quad \text{MPa} \tag{5.11}$$

$$\tau_r = 0.37 + \sigma_n \tan 39° \quad \text{MPa} \tag{5.12}$$

The peak shear strength can be obtained from the first load cycle, and the residual shear strength is from the second to tenth cycles. The friction angle and cohesion as a function of the number of loading cycles are plotted in Figure 5.4. The friction angle and cohesion of all rocks tested rapidly decrease from the first cycle and approached a constant value in the second to tenth cycles. Figure 5.5 shows the shear stress of smooth surfaces as a function of normal stress for 10 cycles. The test results of smooth saw-cut surface well fit to the Coulomb criterion which can be represented by:

for PPSS;

$$\tau_p = 0.04 + \sigma_n \tan 31° \quad \text{MPa} \tag{5.13}$$

for SGR;

$$\tau_p = 0.15 + \sigma_n \tan 35° \quad \text{MPa} \tag{5.14}$$

for SLS;

$$\tau_p = 0.15 + \sigma_n \tan 29° \quad \text{MPa} \tag{5.15}$$

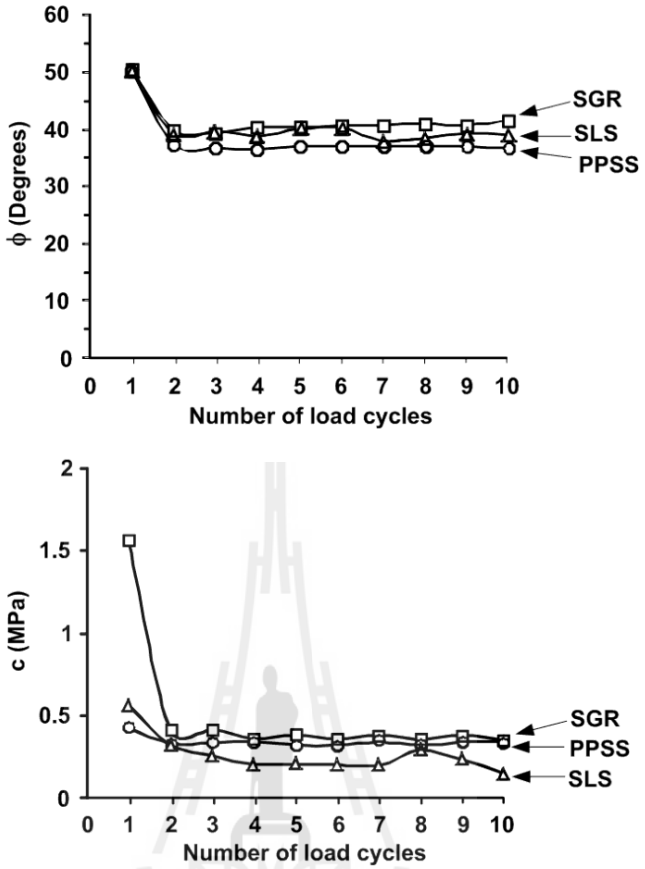

Figure 5.4 Friction angle (ϕ) and cohesion (c) as a function of number of loading cycles for tension-induced fractures.

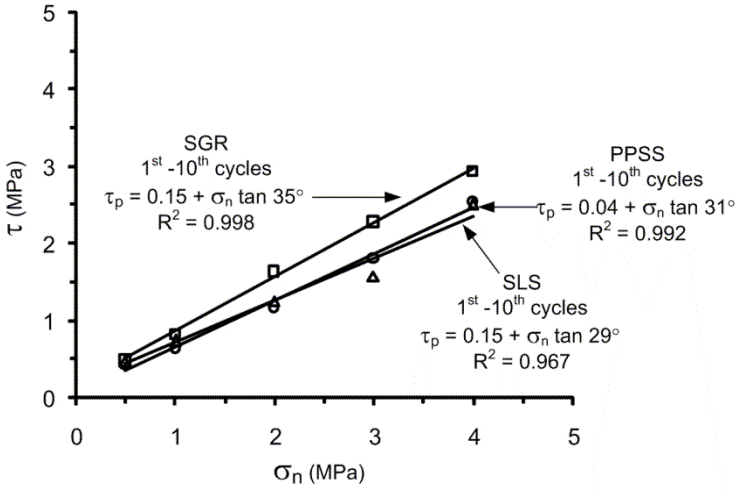

Figure 5.5 Shear strength as a function of normal stress for smooth saw-cut surfaces.

The basic friction angle as a function of the number of load cycles in smooth surface specimens are shown in Figure 5.6. They are slightly lower than those of the residual shear strength. The shearing resistances for the smooth surfaces tend to be independent of the cyclic shearing for the smooth joint.

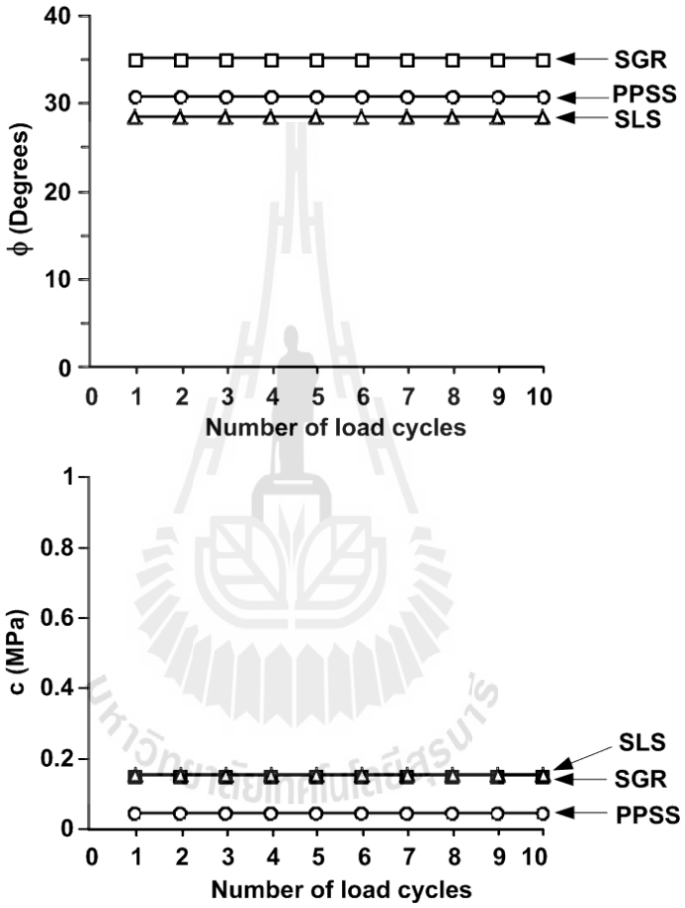

Figure 5.6 Basic friction angle (ϕ) and cohesion (c) of smooth saw-cut surfaces as a function of number of loading cycles.

5.4 Dilation rates as a function of loading cycles

The dilation rates (d_n/d_s) are determined as a function of loading cycle, as shown in Figure 5.7. The decrease of dilation rate is non-linear which can be represented by:

$$d_n/d_s = \alpha \cdot n^{\beta} \tag{5.15}$$

where d_n/d_s is the dilation rate, d_n is the normal displacement, d_s is the shear displacement, n is the number of cycles, and parameters α and β are empirical constants (Table 5.2). As expected the fracture dilation decreases with increasing normal stress and loading cycle.

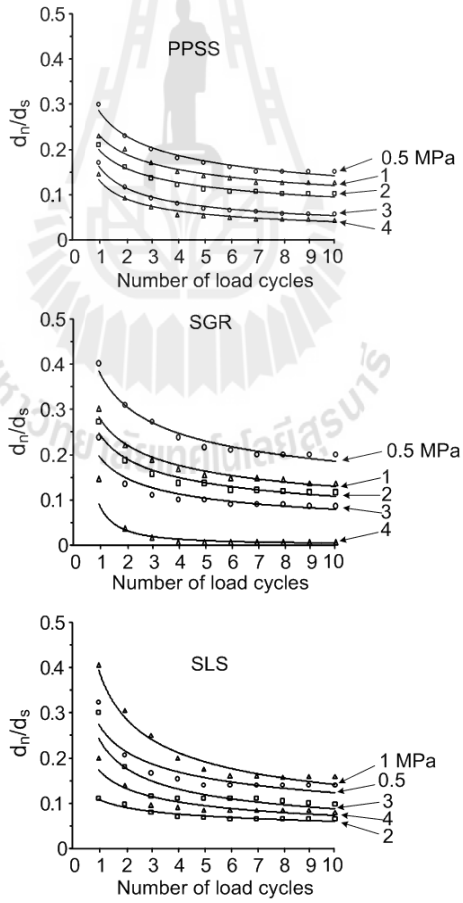

Figure 5.7 Dilation rate of tension-induced fracture as a function of number of load cycles.

Table 5.2 Summary of empirical constants α and β.

σ_n	$d_n/d_s = \alpha \cdot n^{\beta}$								
	PPSS			SGR			SLS		
	α	β	R^2	α	β	R^2	α	β	R^2
0.5	0.287	-0.31	0.974	0.383	-0.31	0.961	0.273	-0.34	0.858
1	0.232	-0.29	0.972	0.281	-0.34	0.969	0.394	-0.44	0.953
2	0.199	-0.33	0.966	0.246	-0.36	0.945	0.107	-0.25	0.919
3	0.162	-0.51	0.986	0.195	-0.40	0.895	0.242	-0.43	0.837
4	0.131	-0.55	0.962	0.089	-1.49	0.870	0.172	-0.37	0.852

Figure 5.8 shows some post-test of PPSS, SGR, SLS, showing that the higher normal stress is applied, the larger sheared off areas are obtained.

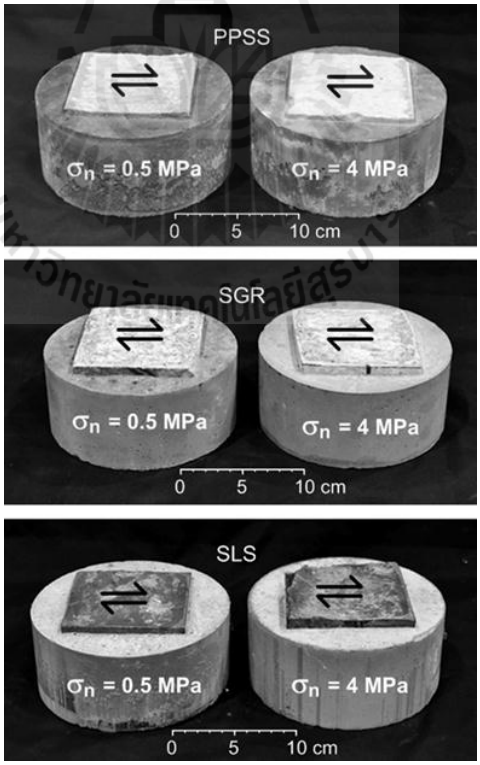

Figure 5.8 Some post-test fracture surfaces.

CHAPTER VI

DISCUSSIONS, CONCLUSIONS, AND RECOMMENDATION FOR FUTURE STUDIES

6.1 Discussions and conclusions

The shear cyclic loading can affect the shear strengths of the tension-induced fractures in the PPSS, SGR and SLS. The decrease of shear strength is affected by the degradation of asperity. As a result the dilation rates of the second to tenth cycle are less than that of the first one for all rock types. The peak shear strength can be obtained from the first loading cycle, and the residual shear strength is from the second to tenth cycles. Here the Coulomb's criterion can well describe the peak and residual shear strengths of the rock fractures. The cohesion and friction angle of all rocks tested rapidly decrease from the first cycle and approach a constant value in the second to tenth cycles. The joint shear stiffness also decreases with increasing loading cycles. The degradation of asperities is the main factor affecting the shear strength of the tension-induced specimens.

The shear strengths of the saw cut surfaces are clearly independent of the loading cycles. This suggests that the effect of cyclic loading is primarily due to the degradation of the rock asperities on the fracture wall. It can therefore be postulated that the cyclic loading effect may be found in other rock types. This supported by the experimental results obtained by Jafari et al. (2003) who conclude that the fracture shear strength will be decreased during cyclic loadings. The number of loading cycles

and normal stress are two main parameters controlling the shearing behaviour of rock joints during cyclic loading. The degradation of asperities is main factors which affect the shear strength of rock joints during large cyclic displacement.

6.2 Recommendations for future studies

The study in this research can be taken as a preliminary guideline and process of study and design. The fracture area should be larger. The shearing rates should be applied at high normal stress and rates, or other forms of testing, such as testing under saturated condition of rock specimen to simulate for rock structure near the wetlands.

REFERENCES

Ahola, M.P., Hsiung, S.M., Kana, D.D. (1996). Experimental study on dynamic behavior of rock joints. In: Stephansson, O., Jing, L., Tsang, C.F. (editors). **Couple Thermo-Hydro-Mechanical Processes of Fractured Media**. Amsterdam, Elsevier: 467–494.

ASTM Standard D5607-08. (2008). Standard test method for performing laboratory direct shear strength tests of rock specimens under constant normal force. In: **Annual Book of ASTM Standards**, American Society for Testing and Materials, West Conshohocken, P.A.

Divoux, P., Boulon, M., and Bourdarot, E. (1997). A mechanical constitutive model for rock and concrete joints under cyclic loading. Rossmanith, H.P. (editors). In **Proceedings of Damage and Failure of Interfaces**, 443-450.

Fox, D.J., Kana, D.D., and Hsiung, S.M. (1998). Influence roughness on dynamic shear behavior in jointed rock. **International Journal of Rock Mechanics & Mining Sciences.** 35: 923–940.

Grasselli, G., and Egger, P. (2003). Constitutive lawfor the shear strength of rock joints based on three-dimensional surface parameters. **International Journal of Rock Mechanics & Mining Sciences.** 40: 25–40.

Hibbeler, R.C. 2011. **Mechanics of Materials**. Person Prentice Hall, United States of America, 32 pp.

Homand, E.F., Lefevre, F., Belem, T., and Souley, M. (1999). Rock joints behavior under cyclic direct shear tests. In: Amadei, B., Kranz, R.L., Scott, G.A., Smeallie, P. (editors). **Rock Mechanics for Industry**. Rotterdam, Balkema: 399–406.

Hosseini, K. A., Pellet, F., Jafari, M. K., and Boulon, M. (2004). Shear strength reduction of rock joints due to cyclic loading. In **Proceedings of the 13th World Conference on Earthquake Engineering** (Paper No. 3070). Vancouver, B.C., Canada, 8 pp.

Hutson, R.W., and Dowding, C.H. (1990). Joint asperity degradation during cyclic shear. **International Journal of Rock Mechanics and Mining Sciences & Geomechanics Abstracts**. 27(2): 109-119.

Itasca (2004). **UDEC 4.0 GUI A Graphical User Interface for UDEC**. Itasca Consulting Group Inc, Minneapolis, Minnesot, 208 pp.

Jaeger, J.C., Cook, N.G.W., and Zimmerman, R.W. (2007). **Fundamentals of Rock Mechanicals**, 4th edition, Australia: Blackwell Publishing, 475 pp.

Jafari, M.K., Pellet, F., Boulon, M., and Hosseini, K.A. (2004). Experimental study of mechanical behavior of rock joints under cyclic loading. **Rock Mechanics and Rock Engineering**. 37 (1): 3–23.

Jafari, M.K., Amini, H. K., Boulon, M., Pellet, F., Jalaly, H., Uromeihy, A., and Buzzy, O. (2002). Laboratory investigation on shear strength variation of joint replicas due to low and high amplitude cyclic displacements. **JSEE**: Summer and Fall. 4(2&3): 37-49.

Jafari, M.K., Amini, H. K., Pellet, F., Boulon, M., and Buzzy, O. (2003). Evaluation of shear strength of rock joints subjected to cyclic loading. **Soil Dynamics and Earthquake Engineering**. 23: 619–630.

Jing, L., Stephansson, O., and Nordlund, E. (1993). Study of rock joints under cyclic loading conditions. **Rock Mechanics and Rock Engineering**. 26(3): 215-232.

Lee, H.S., Park, Y.J., Cho, T.F., and You, K.H. (2001). Influence of asperity degradation on the mechanical behavior of rough rock joints under cyclic shear loading. **International Journal of Rock Mechanics & Mining Sciences.** 38: 967–980.

Ma, M., and Brady, B.H. (1999). Analysis of the dynamic performance of an underground excavation in jointed rock under repeated seismic loading. **Geotechnical and Geological Engineering**. 17: 1–20.

Puntel, E., Bolzon, G., and Saouma, V. E. (2006). A fracture mechanics based model for joints under cyclic loading. **ASCE Journal of Engineering Mechanics.** 132(11): 1151-1159.

Zubelewicz, A., O'Connor, K., Dowding, C.H., Belytschko, T., and Plesha, M.E. (1987). A constitutive model for cyclic behavior of dilatant rock joints. In **Proceedings of the Second International Conference on Constitutive Laws for Engineering Materials**. vol. 2, 1137–1144.

BIOGRAPHY

Mr. Thanakorn Kamonpet was born on September 28, 1987 in Kalasin province, Thailand. He received his Bachelor's Degree in Engineering (Geotechnology) from Suranaree University of Technology in 2009. For him post-graduate, he continued to study with a Master's degree in the Geological Engineering Program, Institute of Engineering, Suranaree university of Technology. During graduation, 2009-2012, he was a part time worker in position of research assistant at the Geomechanics Research Unit, Institute of Engineering, Suranaree University of Technology.